SANDIA REPORT

SAND2004-5585
Unlimited Release
Printed December 2004

Integration of Biological Ion Channels onto Optically Addressable Micro-Fluidic Electrode Arrays for Single Molecule Characterization

Susan M. Brozik, Elizabeth L. Patrick, Jeb H. Flemming, George D. Bachand, and Laura J.D. Frink
Sandia National Laboratories

James A. Brozik, Ryan W. Davis, Lauren A. Meyer, Theodore P. Ortiz, Jason A. Marshall, and David J. Keller
University of New Mexico

Prepared by
Sandia National Laboratories
Albuquerque, New Mexico 87185 and Livermore, California 94550

Sandia is a multiprogram laboratory operated by Sandia Corporation,
a Lockheed Martin Company, for the United States Department of Energy's
National Nuclear Security Administration under Contract DE-AC04-94AL85000.

Issued by Sandia National Laboratories, operated for the United States Department of Energy by Sandia Corporation.

Available to DOE and DOE contractors from
U.S. Department of Energy
Office of Scientific and Technical Information
P.O. Box 62
Oak Ridge, TN 37831

Telephone: (865)576-8401
Facsimile: (865)576-5728
E-Mail: reports@adonis.osti.gov
Online ordering: http://www.osti.gov/bridge

Available to the public from
U.S. Department of Commerce
National Technical Information Service
5285 Port Royal Rd
Springfield, VA 22161

Telephone: (800)553-6847
Facsimile: (703)605-6900
E-Mail: orders@ntis.fedworld.gov
Online order: http://www.ntis.gov/help/ordermethods.asp?loc=7-4-0#online

SAND2004-5585
Unlimited Release
Printed December 2004

Integration of Biological Ion Channels onto Optically Addressable Micro-Fluidic Electrode Arrays for Single Molecule Characterization

Susan M. Brozik, Elizabeth L. Patrick, and Jeb H. Flemming
Microsensors Science and Technology

George D. Bachand
Biomolecular Materials and Interfaces

Laura J.D. Frink
Computational Biology

Sandia National Laboratories
P.O. Box 5800
Albuquerque, NM 87185

James A. Brozik, Ryan W. Davis, Lauren A. Meyer, Theodore P. Ortiz, Jason A. Marshall, and David J. Keller
University of New Mexico, Chemistry Department

Abstract

The challenge of modeling the organization and function of biological membranes on a solid support has received considerable attention in recent years, primarily driven by potential applications in biosensor design. Affinity-based biosensors show great promise for extremely sensitive detection of BW agents and toxins. Receptor molecules have been successfully incorporated into phospholipid bilayers supported on sensing platforms. However, a collective body of data detailing a mechanistic understanding of membrane processes involved in receptor–substrate interactions and the competition between localized perturbations and delocalized responses resulting in reorganization of transmembrane protein structure, has yet to be produced.

This report describes a systematic procedure to develop detailed correlation between (recognition-induced) protein restructuring and function of a ligand gated ion channel by combining single molecule fluorescence spectroscopy and single channel current recordings. This document is divided into three sections: 1. reported are the thermodynamics and diffusion properties of gramicidin using single molecule fluorescence imaging and 2. preliminary work on the $5HT_3$ serotonin receptor. Thirdly, we describe the design and fabrication of a miniaturized platform using the concepts of these two technologies (spectroscopic and single channel electrochemical techniques) for single molecule analysis, with a longer term goal of using the physical and electronic changes caused by a specific molecular recognition event as a transduction pathway in affinity based biosensors for biotoxin detection.

Contents

I. **Introduction**.....**9**

II. **Gramicidin Study:** *The Thermodynamic Properties of Single Ion Channel Formation: Gramicidin*.....**11**

a. **Abstract**.....**11**

b. **Introduction**.....**12**

c. **Experimental**.....**13**

i. Gramicidin Labeling / Materials and Supplies.....13

ii. Reconstitution and Bilayer Formation.....13

iii. Single Molecule Fluorescence Microscopy and Temperature Control.....14

iv. Diffusion / Particle Tracking / Intensity Analysis.....16

d. **Results and Discussion**.....**17**

i. Thermodynamic Analysis from Single Molecule Data.....17

ii. Identifying and Sampling Gramicidin Monomers and Dimers.....18

iii. Temperature Dependence.....20

e. **Summary**.....**22**

f. **Acknowledgements**.....**22**

g. **References**.....**23**

h. **Computational Capabilities for Detailing Structural and Functional Information of Gramicidin Channels**.....**25**

III. **Serotonin Study:** *Combined Single-Molecule Spectroscopic and Single Ion Channel Patch Clamp Measurements of Ligand Gated Ion Channels*.....**27**

a. **Abstract**.....**27**

b. **Introduction**.....**28**

c. **Experimental Section**.....**30**

i. Serotonin Agonist Labeling.....30

ii. Mutagenesis of the $5HT_3$ Serotonin Receptor.....31

iii. Expression of Serotonin Receptor in HEK293-F Cells.....34

d. **Future work**.....**35**

IV. **Transducer Development:** *Design of Miniaturized Electrochemically and Optically-Addressable Platforms for Single Molecule Detection*.....**41**

a. **Abstract**.....**41**

b. **Introduction**.....**42**

c. **Experimental Section**.....**43**

i. Fabrication of Single Molecule Detection Platform using Bosch Process.....43

ii. Fabrication of Single Molecule Detection Platform using Electron Beam Lithography.....44

iii. Fabrication of SMD Platform.....46

d. **References**.....**47**

Figures

Gramicidin Study:

Figure 1 Microscope configuration.....15

Figure 2 Optical orientation of sample relative to the evanescent field is held as an inverted droplet. The lipid bilayer membrane is ~30 Å thick and opposing fluorescent tag are separated by ~58 Å.....16

Figure 3 Scatter plot of raw intensity from ICCD camera vs. measured diffusion coefficient within the membrane. Experiment performed at 21.5°C.....18

Figure 4 Intensity slice of single molecule fluorescence images: (a) is a typical monomer image and (b) is a typical dimer image. Frames integrated for 100 ms.....18

Figure 5 Plot of $\ln\left(K_{eq}^{Conc.}\right)$ vs. $1/T$ 21

Computational Study on Gramicidin:

Figure 1 Comparison of ion and solvent density distributions in a gramicidin channel.....25

Figure 2 Energy barriers experienced by an ion traversing the channel in the presence of an applied electric field.....25

Figure 3 Rod-like inclusion in a lipid bilayer.....26

Serotonin Study:

Figure 1 Serotonin $5HT_3$ receptor incorporated into a lipid bilayer and spectroscopically labeled for single molecule FRET experiments.....28

Figure 2 Plasmid map of the pCDNA3.1-5HT3 construct.....31

Figure 3 Restriction digest of *Bam*HI deletion plasmid.....32

Figure 4 Restriction digest of *Bam*HI mutant plasmid.....33

Figure 5 Double restriction digest of *Bam*HI mutant plasmid.....33

Figure 6 Plasmid map of the 5HT3 His-tagged construct.....34

Transducer Development:

Figure 1 Single molecule detection platform using the Bosch process.....43

Figure 2 Uncut SMD chip showing on-chip working and counter electrodes.....44

Figure 3 Conceptual diagram of side view of SMD platform and relation to objective.....44

Figure 4 Top side (A) and the bottom side (B) of the housing.....45

Tables

Table 1 Temperature Dependent Equilibrium Constantans [a,b], Average Diffusion, and Relative Intensities.....20

Table 2 Standard Thermodynamic Quantities of Reaction at 25^{o} C for $2G_1 \leftrightarrow G_2$.....22

Introduction

Despite decades of intensive research in the field of transmembrane protein function, there is little understanding of the structure-function relationship at the atomic level. This is due to the difficulty of producing sufficient quantities of purified protein for crystallographic studies. To date only a few integral membrane proteins have been resolved at atomic detail. Single molecule spectroscopic measurements, in combination with electrical detection of ion flux, offer an alternative method for obtaining structural and functional information on membrane proteins. Our goal is to develop tools, which allow simultaneous optical and electrical measurements at the single molecule level. In the past couple of years the potential of combined optical and electrochemical measurements applied toward understanding the dynamics of single ion channels has been realized as illustrated by the recent surge of work on the *Shaker* potassium channel and gramicidin ion channel. This LDRD explored the development of unique experimental and computational capabilities for detailing structural and functional information of ligand gated channels; specifically the serotonin type-three receptor. As we built our suite of experimental tools, we used gramicidin as a model system since the helical structure of this peptide had been established and the mechanism of gating through dimerization is generally agreed upon. We began this project by optically detecting dimerization at the single molecule level and have now begun to apply these capabilities toward understanding the $5HT_3$ receptor, a more complicated system. Molecular modeling tools were used to elucidate the mechanism of ion conductance at the atomic level and understand protein lipid interactions. This work will ultimately lead to a prototype device for sensing based on ion transport systems.

Natural ion channels enable active, directional, and preferential transport of ions across an otherwise impermeable cell membrane in response to a specific stimulus. A good example of this is the serotonin type-three receptor that preferentially transports monovalent cations upon binding of serotonin to specific sites on the extracellular domain of the pentameric protein. This binding event causes the movement of 10^6 ions/sec through the channel generating an ion conductance of about 100 pS compared to the leakage conductance of about 0.02 pS. With an amplification factor exceeding 10^6 and a signal to noise ratio exceeding 5000, gated ion channels integrated into a sensor would have the unprecedented ability to detect single binding events. In addition, spectroscopic measurements allow us to measure fast kinetic events and the dynamics

of these transmembrane proteins (TMPs). Unfortunately it has proven extremely difficult to integrate TMPs into a miniaturized device, e.g. a chip-based electrochemical/optical cell, allowing measurement of ion currents and structural states originating from individual ion channels upon response to a target stimulus. We have begun initial design and testing of such a platform enabling real-time analysis and detection of target biological agents.

Gramicidin Study (completed)

The Thermodynamic Properties of Single Ion Channel Formation: Gramicidin

Ryan W. Davis[†], Elizabeth L. Patrick[‡], Lauren A. Meyer[†], Theodore P. Ortiz[†], Jason A. Marshall[†], David J. Keller[†], Susan M. Brozik[‡] and James A. Brozik[†]**

[†]Department of Chemistry, The University of New Mexico, Albuquerque, NM 87131

[‡] Microsensor Science and Technology, Sandia National Laboratories, Albuquerque, NM 87185-0892

Abstract

Single molecule fluorescence imaging has been used to unequivocally differentiate between rhodamine-6G labeled gramicidin monomeric subunits and channel-forming dimers. Absolute identification of individual particles was achieved by accounting for both particle diffusion and intensity, with dimer intensity being twice that of the monomers. In accordance with current diffusion models of proteins in bilayer membranes, we observed dimers to diffuse more slowly through the bilayer than the monomers and have reported diffusion coefficients of 1.2×10^{-8} cm^2 / sec and 3.5×10^{-8} cm^2 / sec for the dimers and monomers respectively. By correlating the diffusion data with measured fluorescence intensities of the tracked particles, it was possible to determine the distribution of monomers and dimers within the bilayer at various temperatures. The results allow complete characterization of the thermodynamic properties of dimer formation, $2G_1 \leftrightarrow G_2$, necessary for channel function. Reported are the temperature dependent equilibrium constants, $\Delta H^{o}_{\text{Reaction}}$, $\Delta G^{o}_{\text{Reaction}}$, and $\Delta S^{o}_{\text{Reaction}}$ for dimer formation in an artificial lipid membrane that has a thickness (30 Å) which is on the same order as the length of the gramicidin channel (26 Å). These experiments compliment and expand single molecule fluorescence methods needed to understand the complexities of ion channel structure / function relationships.

Keywords: Ion Channels, Gramicidin, Single Molecule Fluorescence, and Thermodynamics.

I. Introduction

The identification of specific structural states and the statistical distribution of different structural states of membrane bound proteins in near-native conditions can profoundly affect our understanding of the structural, kinetic, and thermodynamic principles that govern their function. Gramicidin is a 15 amino acid peptide that forms a β-helix in a lipid bilayer [1-3]. Membrane channels can only form after two monomer subunits (G_1) come together to form a head-to-head dimer (G_2) at their N-termini, stabilized by six hydrogen bonds at their dimer junction [1,2,4]. Transmembrane pores that result from dimer formation have been shown to be 26 Å long, 4 Å in diameter, and have a hydrophobic length of ~22 Å [5-7]. Combined fluorescence and electrochemical experiments have shown that the majority of dimers will lead to a channel-forming pore that spans the lipid membrane [8], and allows for an ion flux of $10^6 - 10^7$ ions / sec (monovalent cations; for applied potentials between 150 – 200 mV) [1-3,9]. The gramicidin channel embedded in synthetic lipid bilayer membranes serves as a model system for understanding the basic characteristics of ion channel structure / function relationships, and has been the subject of extensive experimental and theoretical studies [3-8,10-16]. Recently, experiments that combine single molecule fluorescence detection to probe structure and single channel electrical recordings to probe function have suggested subtle structure / function relationships that cannot be observed in the bulk due to ensemble averaging, and suggest multiple conformations in the open and closed states within a lipid bilayer [17,18]. These studies point to the importance of single molecule methods for developing a better understanding of structure / function relationships for membrane bound proteins in general and ion channels in particular.

A necessary condition for channel opening is dimer formation, and the simplest mechanism for closing a channel is by dimer disassociation. Therefore the functionally important process of channel formation is mainly controlled by the equilibrium constant:

$$\underset{}{2G_1} \quad \underset{}{G_2}$$

$$K_{eq}^{SD} = \frac{\left(SD_{G_2} / SD^{o} \right)}{\left(SD_{G_1} / SD^{o} \right)^2} \qquad (1)$$

where SD_{G_2} is the surface density of the dimer, SD_{G_1} is the surface density of the monomer and SD^0 is the standard molar surface density ($SD^0 = 1\,\text{mol} / \text{cm}^2$). The reported equilibrium

constants range from 10^{11} to $>10^{14}$ [8,19]. This large range of values depends largely upon the thickness of the lipid bilayer, but the nature of the bilayer membrane, salt concentration of the surrounding solution, membrane voltage, and cholesterol concentration also play a smaller role on the equilibrium constant [6-8,14,15]. Much of the function of gramicidin ion channels also depends upon their diffusion through and across lipid bilayer membranes. These diffusion rates can vary greatly depending on the temperature (large changes at phase transitions), concentration of cholesterol in the lipid bilayer, and the size of the particle diffusing through the membrane [14,17,20].

In this study we report the thermodynamics and diffusion properties of gramicidin using single molecule fluorescence imaging at several temperature points. The experimental goal is to unequivocally distinguish between individual monomers and dimers and so accurately measure their distributions at various temperatures. After determining the monomer / dimer distribution, it is straightforward to find the temperature dependence of the equilibrium constant ($K_{eq}^{Conc.}$), the standard Gibbs free energy of reaction ($\Delta G^{o}_{\text{Reaction}}$), the standard enthalpy of reaction ($\Delta H^{o}_{\text{Reaction}}$), the standard entropy of reaction ($\Delta S^{o}_{\text{Reaction}}$), and diffusion constants of dimers and monomers.

II. Experimental

(A) Gramicidin Labeling / Materials and Supplies. Literature methods were used to label the gramicidin subunits with Rhodamine-6G on their hydrophilic ends [21]. The labeled gramicidin was then purified with a Sephadex LH-20 size exclusion column (Amersham Biosciences). All organic solvents were reagent grade, purchased from EM Science, and used as received. Gramicidin D (isolated from Bacillus brevis; 80-85 % gramicidin A, 6-7% B, and 5-14% C), triethylamine (TEA), Cholesterol, and Dihexadecyldimethylammonium bromide (DHADAB) were purchased from Aldrich Chemical Company. (5/6)-carboxyrhodamine-6G-(C_6H_{12})-NHS ester was purchased from Molecular Probes Inc. and dimyristoyl-*syn*-glycero-phosphocholine (DMPC) was purchased from Avanti Polar Lipids Inc.

(B) Reconstitution and Bilayer Formation. Gramicidin was reconstituted into lipid vesicles according to Gritsch *et al* [22]. The lipid cake containing labeled gramicidin and 35 mol % cholesterol, was formed by adding 3.08 mg of DMPC, 1.16 mg of cholesterol, 0.57 mg of

DHADAB, and 8.0×10^{-12} mg of labeled gramicidin (a 7.0 μL aliquot of a 5×10^{-7} M stock methanolic solution) to 4 ml of $CHCl_3$. The solution was spun in a round bottom flask at 100 rpm for 25 minutes to homogenize the mixture, followed by rotary evaporation to form the lipid cake, and then overnight vacuum desiccation. Lipid vesicles were reconstituted from the cake by adding 4 ml of 10 mM Tris buffer (pH 7.4) and spinning at 75 rpm and 65° C in a round bottom flask for 30 minutes. The temperature was then decreased to 45° C and the mixture spun for 2 hours. Finally, the temperature was increased to 60° C and spun for an additional 45 minutes. The reconstituted vesicles were then cycled through five consecutive freeze-thaw cycles (-198° C to 50° C), followed by vesicle extrusion with a mini-extruder (Avanti Polar Lipids Inc.) equipped with a 0.4 μm pore diameter polycarbonate membrane. The final labeled gramicidin concentrations were verified by UV-vis spectroscopy from a standard calibration curve derived from known concentrations of rhodamine-6G.

Samples for single molecule particle tracking experiments were prepared on high index of refraction (1.78) flint glass coverslips (Olympus Inc.), cleaned with concentrated sulfuric acid followed by extensive rinsing with nanopure (18 GΩ) water, dried under a stream of dry nitrogen, and UV-ozonated for 30 minutes prior to use. Gramicidin incorporated lipid bilayers were formed on the prepared flint glass substrates by the vesicle fusion / adsorption / collapse technique described by Brian and McConnell and characterized by Leonenko *et al* [23,24]. Assuming 100% incorporation of gramicidin into the membrane [25] and using the facts that each lipid molecule occupies a 0.6 nm^2 area at the surface of the membrane [26,27] and that the lipid bilayer is 3 nm thick (bilayer thickness was measured by ellipsometry; Gaertner L116SF / Gaertner Scientific Corp.), the total concentration of gramicidin subunits, $[G_0]$, in the membrane is calculated to be 1.17 μM, with a total surface density of 3.50×10^{-16} mol / cm^2 in the present study. The hydrophobic region of the lipid bilayer used in this study was previously measured using electrical impedance spectrometry and found to be 2.8 nm [28,29].

(C) Single Molecule Fluorescence Microscopy and Temperature Control. The microscope used in the single molecule fluorescence studies is depicted in Figure 1. In this apparatus the beam from a doubled cw-Nd:YAG laser (532 nm, 10 mW, BWTEK Inc.) is passed through a 532 nm laser line filter (±2 nm FWHM, OptoSigma Corp.), a calcite polarizer, and a ¼ waveplate to produce a clean circularly polarized beam. The beam is then passed through a spatial filter,

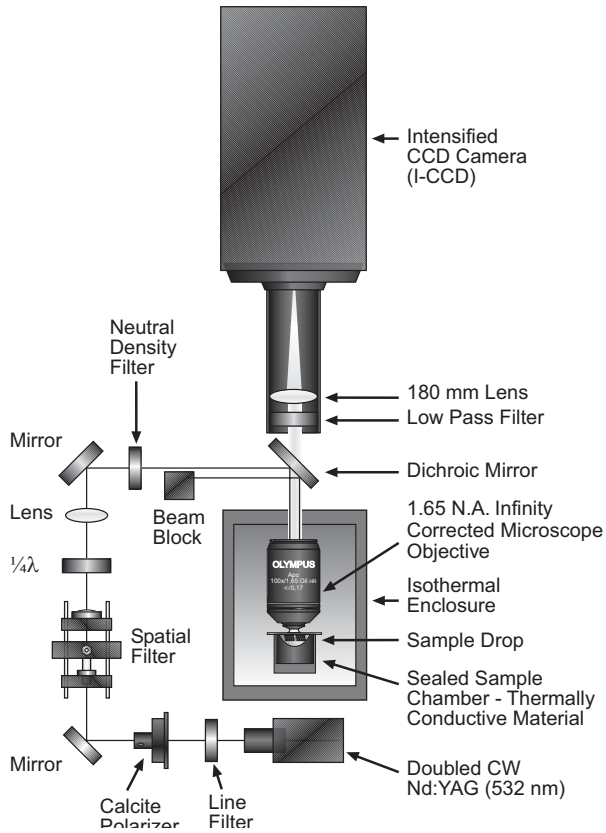

Figure 1. Microscope configuration. 532 nm excitation produced by a Nd:YAG laser and attenuated to ~1 mW. Single molecule fluorescence collected by a 1.65 N. A. infinity corrected microscope objective. Single molecule images collected with an ICCD camera operating at a 100 ms frame rate.

attenuated to 1 mW with a neutral density filter, and focused on the back of the microscope objective with a 500 mm focal length quartz lens. The focused beam is directed onto the edge of a 1.65 N.A. infinity corrected microscope objective (Olympus Inc.) with a dichroic mirror (QS4SLP, Chroma Technologies Corp.) such that the deflected beam is totally internally reflected at the flint glass / water interface. Figure 2 shows the orientation of the exciting evanescent field to the sample incorporated within the lipid bilayer. The size of the laser beam at the glass / water interface was 6 μm^2. Fluorescence from a single labeled gramicidin monomer or dimer was collected through the microscope objective, passing through the dichroic mirror, filtered with a long pass filter (HQ550LP, Chroma Technologies Corp.) to remove scattered laser light, and imaged on an intensified CCD camera (IPentaMax, Roper Scientific Inc.) with a quartz lens. Fluorescence from single molecules yielded diffraction limited spots (~250 nm) that covered a 6x6 area of pixels on the ICCD camera (FWHM).

The sample was inverted relative to the flint glass cover slip and sealed around a chamber with thermally conducting walls to prevent evaporation and maintain thermal equilibrium with the isothermal enclosure that surrounded the sample. The temperature within the isothermal enclosure was set and maintained with a combination of a thermostat and a ceramic heating element. The temperature within the isothermal enclosure was measured with a J-type thermocouple mounted in near contact with the sample. For the temperature dependent

experiments the concentration was fixed at 1.17 μM and the temperature changed from 21.5° C to 33.2° C in seven nearly equal steps.

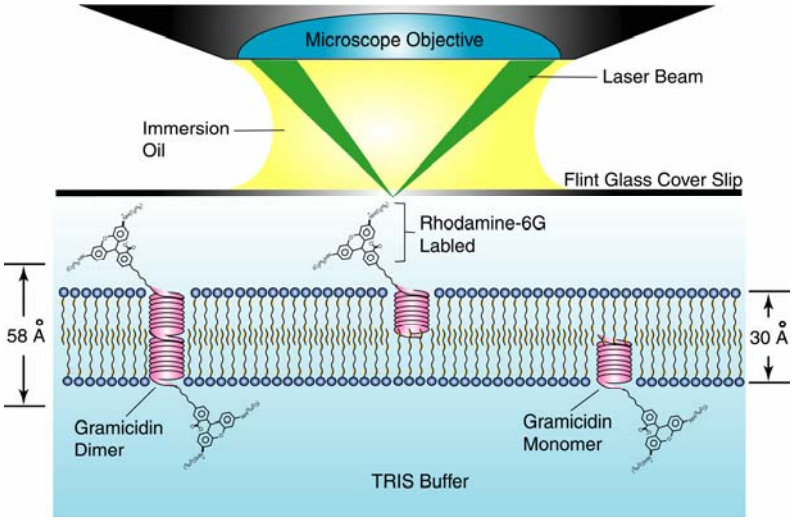

Figure 2. Optical orientation of sample relative to the evanescent field is held as an inverted droplet. The lipid bilayer membrane is ~30 Å thick and opposing fluorescent tag are separated by ~58 Å.

(D) Diffusion / Particle Tracking / Intensity Analysis. Image recording and single molecule tracking was aided by the WinView software package supplied by Roper Scientific in tandem with a custom made C program. Individual mean-square displacements were based upon equation 2,

$$\overline{r}^2(t) = \sum_{t-t_0} \left| r(t) - r(t - t_0) \right|^2 \qquad (2)$$

where $\overline{r}^2(t)$ is the mean square displacement, $r(t)$ is the position vector at time t, and $t_0 = 0.1\,\text{sec}$ is the frame rate from the data acquisition. The lateral diffusion constant (D) is then related to the mean square displacement by:

$$\overline{r}^2(t) = 4Dt \qquad (3)$$

From equation 3, the diffusion constant of individual particles was determined by plotting $\overline{r}^2$ vs. time for the entire trajectory of tracked single particles. The lateral diffusion coefficients of each particle were then determined from the slope of these lines.

The average intensity for each tracked particle was derived from the gaussian fluorescence peak of the individual particles in each frame. The reported intensity is the average over such peak intensities in all frames for the individual particles.

III. Results and Discussion

(A) Thermodynamic Analysis from Single Molecule Data. The thermodynamic properties were determined from the measured distribution of monomers vs. dimers within the lipid membrane. The equilibrium constant for dimer formation, expressed in terms of molar concentrations, is

$$K_{eq}^{Conc.} = \frac{\left([G_2] / C^{o} \right)}{\left([G_1] / C^{o} \right)^2} \tag{4}$$

where C^o = 1 mol / L is the standard molar concentration. The fractional populations of the monomers and dimers are defined as:

$$f(G_1) = \frac{\text{number of } G_1\text{'s counted}}{\text{total number of particles counted}} \tag{5}$$

$$f(G_2) = \frac{\text{number of } G_2\text{'s counted}}{\text{total number of particles counted}} \tag{6}$$

If $[G_0]$ is the total concentration of gramicidin subunits, then:

$$f(G_2) = \frac{[G_2]}{[G_0] - [G_2]} \tag{7}$$

and

$$[G_2] = \frac{f(G_2)[G_0]}{(1 + f(G_2))} \tag{8}$$

$$[G_1] = [G_0] - 2[G_2] \tag{9}$$

Therefore equilibrium constants can be determined from single molecule fluorescence data by identifying and counting single particles.

The standard enthalpy of reaction, $\Delta H^{o}_{\text{Reaction}}$, can then be determined by measuring the temperature dependence of the equilibrium constant over a small, but reasonable, temperature range, using the van't Hoff equation

$$\ln\left(\frac{K_{eq}^{Conc.}(T_2)}{K_{eq}^{Conc.}(T_1)}\right)=\frac{-\Delta H^{o}_{\text{Reaction}}}{\text{R}}\left(\frac{1}{T_2}-\frac{1}{T_1}\right), \qquad (10)$$

and the entropy of reaction can be found from equation (11):

$$\Delta G^{o}_{\text{Reaction}}(T)=-R(T)\ln K(T)=\Delta H^{o}_{\text{Reaction}}(T)-T\Delta S^{o}_{\text{Reaction}}(T). \qquad (11)$$

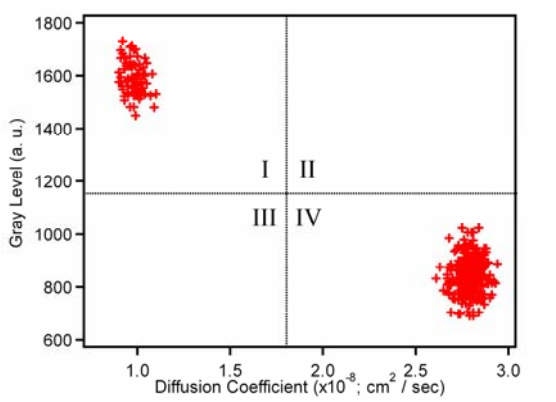

Figure 3. Scatter plot of raw intensity from ICCD camera (in arbitrary gray scale) vs. measured diffusion coefficient within the membrane. Experiment performed at 21.5°C.

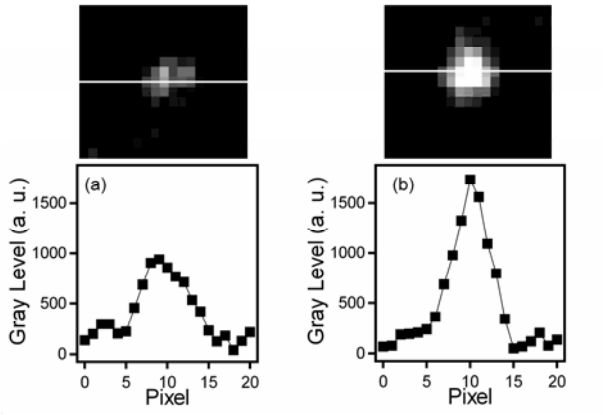

Figure 4. Intensity slice of single molecule fluorescence images: (a) is a typical monomer image and (b) is a typical dimer image. Frames integrated for 100 ms.

(B) Identifying and Sampling Gramicidin Monomers and Dimers. Gramicidin dimers can be clearly distinguished from gramicidin monomers by both fluorescence intensity and diffusion coefficient. Figure 3 shows clear, well-separated clusters, and high correlation between brightness and diffusion coefficient: dim particles diffuse fast, bright particles diffuse more slowly, as expected if the dim particles are monomers and the bright particles are dimers. Furthermore, two-step photobleaching and photoblinking has been observed for a small number of particles that fall into region I of figure 3, providing additional evidence that the bright, slow diffusing particles are dimers. No two-step photobleaching or photoblinking was observed for particles that fall into region IV of figure 3. As shown in figure 4, bright particles are almost twice as intense as dim particles, again consistent with their identity as dimers. It should be

noted that since a dimer is nearly 30 Å in length and the hydrocarbon linker attached to the fluorescent tag is an additional 14 Å, then the fluorescent tags are separated by up to 58 Å, much longer than the Förster radius for rhodiame-6G pairs (Förster radius ≈ 20 Å). Self-quenching of opposing dyes should thus be minimal. It is known, through Stokes-Einstein's law of diffusion, that particles with larger sizes will move more slowly through a viscous medium than particles with smaller sizes because of their increased drag. A lipid bilayer is not an isotropic medium but is rather anisotropic and gramicidin dimers are more like cylinders rather than like spheres. Therefore one would not expect the diffusivity to have an exactly inverse relationship to the size of the particle, but the inverse trend will hold approximately [20,30-33.]. The measured diffusion coefficients at 25^{o} C are 1.2x10^{-8} and 3.5x10^{-8} cm^{2} / sec for the dimer and monomer respectively (diffusion coefficients are summarized in table 1). It should also be noted that the particles that diffuse quickly, identified as gramicidin monomers, have a near Gaussian distribution. This effectively eliminates the possibility that the bilayer leaflet in closest proximity to the flint glass substrate is significantly less mobile than the opposing leaflet. If the mobility of the two leaflets were significantly different one would expect two separate and distinct distributions for monomer particles. Using fluorescence recovery after photobleaching, Tank *et al* reported diffusion constants for the gramicidin dimer embedded in DMPC lipid bilayers and recorded at a variety of temperatures and cholesterol concentrations. At 35 mol % of cholesterol and 25^{o} C, they reported a diffusion constant of ~1x10^{-8} cm^{2} / sec which is very close to our measured value under similar sample conditions [14]. Furthermore our reported monomer diffusion is also in agreement with that measured by Borisenko *et al* from a previous single molecule study (3.3x10^{-8} cm^{2} / sec) in a lipid bilayer composed of dioleoylphosphatidylcholine [17]. While measuring either the relative fluorescence intensities or the diffusivity are by themselves good methods for identifying the particles, it becomes a much more convincing argument if the two can be correlated. Such a correlation is displayed in figure 3 and the bimodal distribution of the fluorescence intensity with particle diffusivity allows one to unequivocally categorize the particles as either monomers or dimers. Hence, the particles that fall into region I are dimers and those in region IV are monomers (figure 3). From this distribution the equilibrium constants can be determined as described in the preceding section. The measured equilibrium constants are collected in table 1.

Table 1. Temperature Dependent Equilibrium Constantans [a,b], Average Diffusion, and Relative Intensities

Temp (°C)	$K_{eq}^{Conc.}(T)$ (x10^5)	D_{G_1} (x10^{-8} cm^2 / sec)	D_{G_2} (x10^{-8} cm^2 / sec)	G_1 Intensity (Gray Level, a. u.) [c]	G_2 Intensity (Gray Level, a. u.) [c]
21.5	2.70	2.8 ± 0.1	0.96 ± 0.05	830	1589
22.7	2.51	3.5 ± 0.1	1.2 ± 0.09	951	1774
25.4	2.12	3.5 ± 0.1	1.2 ± 0.1	942	1912
26.7	1.81	3.6 ± 0.1	1.2 ± 0.09	890	1746
28.2	1.57	3.7 ± 0.1	1.1 ± 0.1	944	1834
31.0	1.31	3.8 ± 0.1	1.1 ± 0.1	895	1698
33.2	1.26	4.1 ± 0.1	1.2 ± 0.1	921	1779

[a] Total membrane concentration = $[G_0] = [G_1] + 2[G_2] = 1.17\text{x}10^{-6}$ M

[b] $K_{eq}^{Conc.}$ given by equation (4).

[c] Gray level depends on intensifier gain setting. Different temperature points were taken on separate days and the intensifier was optimized each day, which leads to slightly different gray levels between temperature points.

(C) Temperature Dependence. Depicted in figure 5 is a plot of $\ln\left(K_{eq}^{Conc.}\right)$ vs. $1/T$ from experimental equilibrium constant data (the circles). From the slope, $\Delta H^{o}_{\text{Reaction}} = -53.0\ kJ/mol$; the formation of the dimer is thus an exothermic process as expected. Moreover since the energy of a typical hydrogen bond is between 8-10 *kJ / mol*, the measured $-\Delta H^{o}_{\text{Reaction}}$ is consistent with the model proposed by Urry *et al* in which the dimer involves the formation of six hydrogen bonds [1,4]. The value of $\Delta H^{o}_{\text{Reaction}}$ compliments the results of Bamberg and Läuger who determined that the formation of a gramicidin dimer embedded in a 50 Å thick lipid matrix was an endothermic process with $\Delta H^{o}_{\text{Reaction}} = +13.4\ kJ/mol$ [34]. In that earlier study, the authors concluded that, because the membrane was considerably thicker than a gramicidin dimer, the energy liberated by the formation of six hydrogen bonds (an exothermic process) was more than compensated by the energy required to distort the lipid matrix (an endothermic process). Thus making the overall process endothermic. In the present study, the lipid thickness (30 Å) and the length of the dimer (26 Å) are approximately matched. Moreover, the length of the hydrophobic region (22 Å) [6,7] of the gramicidin dimers also approximately matches the hydrophobic region of the lipid bilayer (28 Å) [28,29], so one would not expect such a severe distortion of the lipid matrix

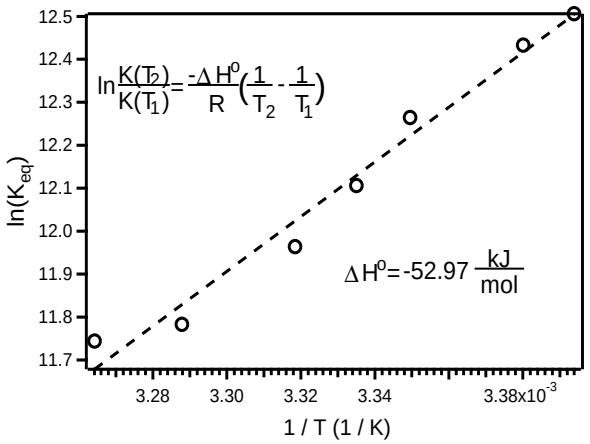

Figure 5. Plot of $\ln\left(K_{eq}^{Conc.}\right)$ vs. $1/T$.
Circles are the experimental data and the dashed line is a linear fit of the data to the van't Hoff equation (equation (10)).

upon dimer formation. The measured $\Delta H^{o}_{\text{Reaction}}$ in the current study should therefore more closely reflect the intrinsic enthalpy of dimer formation irrespective of the lipid bilayer. The measured $K_{eq}^{SD}\left(25^{o}\text{ C}\right)$ value agrees with the observations made by Veatch *et al.* over 20 years ago when they observed that $K_{eq}^{SD}\left(25^{o}\text{ C}\right)\geq 10^{14}$ for a membrane that was 31 Å thick [8]. From the measured equilibrium constant, $\Delta G^{o}_{\text{Reaction}}$ has a value of –30.4 *kJ / mol*. Finally, from $\Delta H^{o}_{\text{Reaction}}$ and $\Delta G^{o}_{\text{Reaction}}$, $\Delta S^{o}_{\text{Reaction}}$ has a value of –75.8 *J / mol K*. Assuming that the major contribution to $\Delta S^{o}_{\text{Reaction}}$ is associated with the translational degrees of freedom ($\Delta S^{o}_{\text{Reaction}} \approx \Delta S^{o}_{\text{Reaction, trans}}$), one can estimate $\Delta S^{o}_{\text{Reaction}}$ from pure translational partition functions for monomers and dimers [35]:

$$\Delta S^{o}_{\text{Reaction, trans}} = k\ln\left(\frac{2t}{e}\Lambda_{G_1}^{2}C_{3D}^{o}\right) \qquad (12)$$

where k is Boltzmann's constant, t is the thickness of the membrane, $\Lambda_{G_1}^{2}=\frac{h^2}{2\pi mkT}$, m is the mass of a gramicidin monomer, and C_{3D}^{o} is the standard molar concentration in units of molecules/m^3. With t = 3 nm, m = 3.13x10^{-24} Kg, and $C_{3D}^{o}=1M=6.02x10^{26}$ molecules/m^3, equation 12 yields $\Delta S^{o}_{\text{Reaction, trans}}=-98.4\ J/mol\ K$. The close correlation between measured and calculated values suggests that the negative change in standard entropy of reaction is primarily due to the loss of translational freedom upon dimerization and the different masses of monomers vs. dimers, with only minor contributions from the lipid membrane and other degrees of freedom associated with the products and reactants. The thermodynamic data are collected in table 2.

Table 2. Standard Thermodynamic Quantities of Reaction at 25° C for $2G_1 \leftrightarrow G_2$

ΔH^o (kJ / mol)	$K_{eq}^{Conc.}\left(T = 25^o\ C\right)$	$K_{eq}^{SD}\left(T = 25^o\ C\right)$ [a,b]	ΔG^o (kJ / mol)	ΔS^o (J / mol K)
-53.0	2.09 x 10^5	6.86 x 10^{14}	-30.4	-75.8

[a] Total Surface Density $= SD_{G_0} = SD_{G_1} + 2SD_{G_2} = 3.50 \times 10^{-16}$ mol/cm^2 [b] K_{eq}^{SD} given by equation (1).

IV. Summary

Without question gramicidin in artificial lipid bilayers has become the most important model system for the study of membrane bound ion channels in biological systems and has been the subject of intense study for at least 30 years. In that time there have been many well-formulated studies involving single channel electrical recordings and ensemble spectroscopic measurements (NMR and fluorescence). These studies have been used to elucidate structure, function, rates of channel formation, ion flux, the thermodynamic properties of the transition state, etc. Even so, the basic thermodynamic properties (standard enthalpy, Gibbs free energy, and entropy of reaction) have never been measured. This is due in part to the large equilibrium constant for dimer formation (the chemical reaction responsible for "turning on" the ion channel) and the lack of the necessary tools needed to directly measure the equilibrium constant. In this study we have directly measured the standard free energy of reaction and the standard enthalpy of reaction using single molecule fluorescence techniques to unequivocally distinguish monomers from dimers and hence have directly measured their absolute distribution in a lipid bilayer at different temperatures. In addition, this work has made use of rigorous thermodynamic arguments to augment the experimental results. In short the study presented above uses new state of the art fluorescence techniques to address a fundamental problem in an important model system.

Acknowledgements: The authors would like to acknowledge grants from NIH (GM63808) and Sandia National Laboratories for partial support of this research. Sandia is a mulitprogram laboratory operated by Sandia Corporation, a Lockheed Martin Company, for the United States Department of Energy's National Nuclear Security Administration under Contract DE-AC04-94AL85000. The University of New Mexico and Sandia National Laboratories are also thanked for programmatic support.

References:

(1) Koeppe, R. E., II; Andersen, O. S. *Annual Review of Biophysics and Biomolecular Structure* **1996**, *25*, 231.

(2) Woolley, G. A.; Wallace, B. A. *Journal of Membrane Biology* **1992**, *129*, 109.

(3) Anderson, O. S.; Apell, H. J.; Bamberg, E.; Busath, D. D.; Koeppe, R. E., II; Sigworth, F. J.; Szabo, G.; Urry, D. W.; Woolley, G. A. *Nature Structural Biology* **1999**.

(4) Urry, D. W.; Goodall, M. C.; Glickson, J. D.; Mayers, D. F. *Proceedings of the National Academy Sciences USA* **1971**, *68*, 1907.

(5) Urry, D. W. *Proceedings of the National Academy Sciences USA* **1971**, *68*, 672.

(6) Elliott, J. R.; Needham, D.; Dilger, J. P.; Haydon, D. A. *Biochemica et Biophysica Acata* **1983**, *735*, 95.

(7) Huang, H. W. *Biophysical Journal* **1986**, *50*, 1061.

(8) Veatch, W. R.; Mathies, R.; Eisenberg, M.; Stryer, L. *Journal of Molecular Biology* **1975**, *99*, 75.

(9) O'Connell, A. M.; Koeppe, R. E., II; Andersen, O. S. *Science* **1990**, *250*, 1256.

(10) Bamberg, E.; Apell, H. J.; Alpes, H. *Proceedings of the National Academy Sciences USA* **1977**, *74*, 2402.

(11) Bamberg, E.; Apell, H. J.; Alpes, H.; Gross, E.; Morell, J. L.; Harbaugh, J. F.; Janko, K.; Lauger, P. *Federation Proceedings* **1978**, *37*, 2633.

(12) Szabo, G.; Urry, D. W. *Science* **1979**, *203*, 55.

(13) Weinstein, S.; Wallace, B. A.; Blout, E. R.; Morrow, J. S.; Veatch, W. R. *Proceedings of the National Academy Sciences USA* **1979**, *76*, 4230.

(14) Tank, D. W.; Wu, E. S.; Meers, P. R.; Webb, W. W. *Biophysical Journal* **1982**, *40*, 129.

(15) Schagina, L. V.; Blasko, K.; Grinfeldt, A. E.; Korchev, Y. E.; Lev, A. A. *Biochimica et Biophysica Acta* **1989**, *978*, 145.

(16) Chernyshev, A.; Cukierman, S. *Biophysical Journal* **2002**, *82*, 182.

(17) Borisenko, V.; Lougheed, T.; Hesse, J.; Fureder-Kitzmuller, E.; Fertig, N.; Behrends, J. C.; Woolley, G. A.; Schutz, G. J. *Biophysical Journal* **2003**, *84*, 612.

(18) Harms, G. S.; Orr, G.; Montal, M.; Thrall, B. D.; Colson, S. D.; Lu, H. P. *Biophysical Journal* **2003**, *85*, 1826.

(19) Rokitskaya, T. I.; Antonenko, Y. N.; Kotova, E. A. *Biochemica et Biophysica Acata* **1996**, *1275*, 221.

(20) Saffman, P. G.; Delbruck, M. *Proceedings of the National Academy Sciences USA* **1975**, *72*, 3111.

(21) Lougheed, T.; Borisenko, V.; Hand, C. E.; Woolley, G. A. *Bioconjugate Chemistry* **2001**, *12*, 594.

(22) Gritsch, S.; Nollert, P.; Jaehnig, F.; Sackmann, E. *Langmuir* **1998**, *14*, 3118.

(23) Leonenko, Z. V.; Carnini, A.; Cramb, D. T. *Biochimica et Biophysica Acta* **2000**, *1509*, 131.

(24) Brian, A. A.; McConnell, H. M. *Proceedings of the National Academy Sciences USA* **1984**, *81*, 6159.

(25) Bransburg-Zabary, S.; Kessel, A.; Gutman, M.; Ben-Tal, N. *Biochemistry* **2002**, *41*, 6946.

(26) Cevc, G.; Marsh, D. *Phospholipid Bilayers*; Wiley and Sons: New York, 1987.

(27) Nagle, J. F.; Tristram-Nagle, T. *Biochemica et Biophysica Acata* **2000**, *1469*, 159.

(28) Branch, D. W.; Brozik, S. M.; Hughes, R. C. *SAND2001-2792A* **2001**, 1.

(29) Hughes, R. C.; Branch, D. W.; Brozik, S. M. *SAND2003-0116* **2003**, 1.

(30) Cohen, M. H.; Turnbull, D. *Journal of Chemical Physics* **1959**, *31*, 1164.

(31) Traeuble, H.; Sackmann, E. *Journal of the American Chemical Society* **1972**, *94*, 4499.

(32) Galla, H. J.; Hartmann, W.; Theilen, U.; Sackmann, E. *Journal of Membrane Biology* **1979**, *48*, 215.

(33) Ke, P. C.; Naumann, C. A. *Langmuir* **2001**, *17*, 3727.

(34) Bamberg, E.; Lauger, P. *Biochemica et Biophysica Acata* **1974**, *367*, 127.

(35) McQuarrie, D. A. *Statistical Mechanics*, 1 ed.; HarperCollinsPublishers: New York, 1976.

Computational Capabilities for Detailing Structural and Functional Information of Gramicidin Channels

Laura Frink, Sandia National Laboratories

We report work on modeling ion transport through gramicidin A using molecular theory (specifically density functional theory - DFT) based tools. Figure 1 compares ion and solvent density distributions in a gramicidin A channel where there is no electrochemical potential gradient across the membrane. The upper two panels show a calculation done with a Poisson-Boltzman electrolyte (point charge ions in a continuum dielectric solvent). The bottom three panels show a calculation done with a 3 component electrolyte where the ions and solvent all have finite size. These calculations were based on the 1MAG protein data bank structure of gramicidin A. In addition to density distributions, DFT was used to predict the energy barriers experienced by an ion traversing the channel in the presence of an applied electric field (Figure 2), assess the possibility of multiple occupancy of ions in the channel, and compute ion flux through the channel. In addition, this DFT code has been extended to treat polymer fluids.

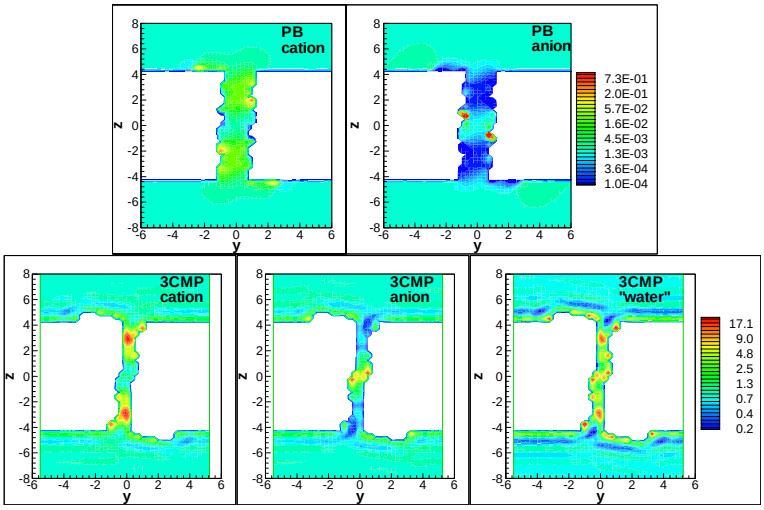

Figure 1. Comparison of ion and solvent density distributions in a gramicidin A channel

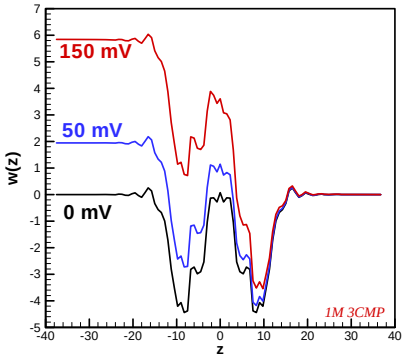

Figure 2. Energy barriers experienced by an ion traversing the channel in the presence of an applied electric field

We are currently investigating gramicidin dissociation in lipid bilayers. The first challenge was to model the lipid layers. We have been successful in understanding how to make a coarse-grained bilayer, and more importantly how to choose parameters that will optimize the model with respect to the physics of the real

lipids of interest. The particular model lipid molecule we have been working has an 8-2-8 architecture with the 8 bead chains representing the tails and the 2-bead segment representing the head group. Each of the tail beads can be thought of as approximately two CH_2 groups. The head group beads are larger than the tail beads in order to ensure that bilayers are in a stable phase. The interaction parameters (solvent-head, solvent-tail, solvent-solvent, head-head, head-tail, tail-tail) can all be varied to optimize bilayer properties. We have been focusing to date on the degree to which the chains are stretched (an alternate way to think of bilayer thickness that is model independent), and the density of the lipids in the bilayer. Most recently we have implemented both branched chains in the DFT code and the ability to treat charged groups on the chain in order to drive the lipid models more in the direction of atomistic (not quite so coarse grained) models. We will ultimately need this because the hydrophobicity of the proteins is based mostly on charge distribution (our current coarse grained models drive bilayer assembly through van der Waals effects alone). We will need an adequate model of charge distribution across the membrane as well.

Finally, we have performed demonstration calculations for a simple rod-like inclusion in a lipid bilayer (a 2-dimensional calculation) to demonstrate that the molecular theory approach can capture the effect of the inclusion on both the bilayer-water interface, and the local lipid tail structure in the vicinity of the inclusion (Figure 3).

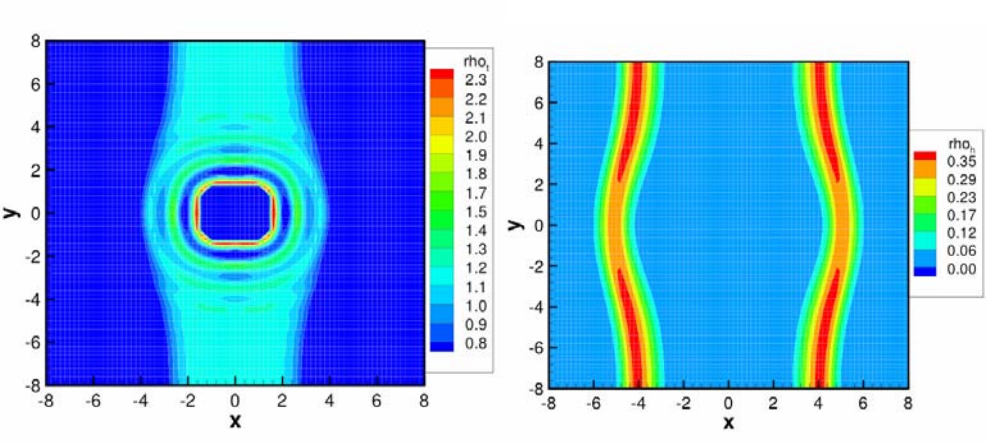

Figure 3. Rod-like inclusion in a lipid bilayer.

Serotonin (work in progress)

Combined Single-Molecule Spectroscopic and Single Ion Channel Patch Clamp Measurements of Ligand Gated Ion Channels

Ryan W. Davis[†], Elizabeth L. Patrick[‡], Jeb H. Flemming[‡], George D. Bachand[‡], Susan M. Brozik[‡] and James A. Brozik[†]**

[†]Department of Chemistry, The University of New Mexico, Albuquerque, NM 87131

[‡] Microsensor Science and Technology, Sandia National Laboratories, Albuquerque, NM 87185-0892

Abstract

The technical goal of this component of the work was to insert a 6x Histidine (His)-tag at the C-terminus end of the serotonin receptor such that recombinant protein could be purified by Ni-NTA chelate chromatography and to fluorescently label serotonin receptor agonists. We report the mutagenesis of the serotonin receptor and expression into HEK293-F cells. Procedures for purification are described once stable expression is achieved. Fluorophores with and without covalent spacers to the indole nitrogen have been chemically attached, as it is believed that the primary amine and alcohol groups are responsible for ligand binding to the serotonin receptor. Spectroscopic studies will be carried out to determine the number of labeled ligands bound to the purified receptor thus detailing the number of receptor sites for serotonin.

I. Introduction

Many of the cell membrane functions such as regulation of cellular potential, selective filtration, and regulation of nutrient and waste movement are mediated by transmembrane proteins. TMPs span the lipid bilayer, requiring hydrophobic regions that penetrate the membrane and hydrophilic regions that are exposed to the aqueous medium on either side. An important class of TMPs form pores or channels enabling active, directional, and preferential transport of ions across the otherwise impermeable membrane in response to a specific stimulus. A good example is the serotonin type-three receptor that preferentially transports monovalent cations upon binding of serotonin to specific sites on the extracellular domain of the pentameric protein.

All serotonin receptors are G-coupled proteins except for the $5HT_3$ receptor, which acts as a ligand gated ion channel. Other members of this family of channels include glycine receptors, binding inhibitory neurotransmitters and receptors for excitatory neurotransmitters (acetylcholine and serotonin). The nicotinic acetylcholine receptor is the best characterized to date but very limited structural information is available for the other ligand-gated channels primarily due to the challenges of obtaining large enough quantities of purified protein for experimental characterization. The $5HT_3$ receptor is a homopentameric transmembrane protein that has four transmembrane domains (predicted, for each subunit) and functions by allowing both K^+ and Na^+ to flow across a synaptic membrane upon a ligand binding event. The goal of this project was to obtain a dynamic view of the molecular architecture for a single $5HT_3$ serotonin receptor. This project is still in its infancy and the work conducted thus far is reported. Utilizing a mammalian expression system, we will obtain purified $5HT_3$ receptor as well as mutant receptors and reconstitute into lipid bilayers for single channel analysis. Specifically, single-

Figure 1. Serotonin $5HT_3$ receptor incorporated into a lipid bilayer and spectroscopically labeled for single molecule FRET experiments.

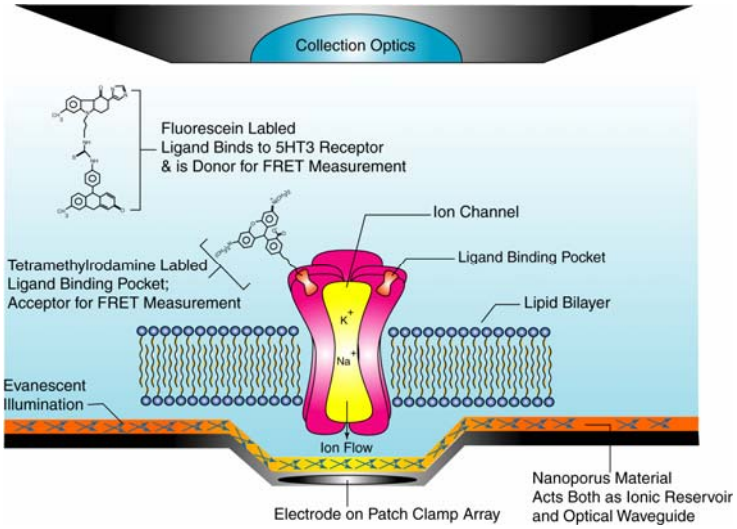

molecule methods will be used to get a dynamic view of structure and function as well as probing the local chemical environments of both the receptor and agonist. Such a view will necessarily correlate ligand binding to structural changes and channel opening, revealing the precise mechanistic sequence of events that determine the operation of ion channel proteins. Fluorescence spectroscopy will be used to excite fluorescent molecules that have been carefully labeled on the subunits of the serotonin receptor (similar experiments as described earlier in the gramicidin study). Alternatively, a micro patch clamp array with a built-in optical access can be used (Figure 1). The design of this chip based analytical tool is described in the following section.

Here we report our initial work on designing mutated serotonin receptor and expression in HEK293-F cells as well as the fluorescent labeling of serotonin receptor agonists. Experimental characterization of the ligand gated channel system was not conducted during the LDRD funding period, however we have begun this work in this fiscal year (FY05) under new funding. Future work to be conducted includes several types of optical experiments undertaken in conjunction with patch clamp electrochemical measurements. Our approach will synchronize electrochemical and spectroscopic measurements by fluorescently labeling the agonists thereby directly measuring the binding event followed by conformational changes and commensurate functioning of the gate (using labeled ions and site specific labeling of the channel/gate). Such a methodology will give direct kinetic and mechanistic information about the biochemical function of the ligand-gated receptor. Fluorescence resonance energy transfer (FRET) is highly dependent on the distance separating conjugate donor / acceptor pairs and can be used as a "molecular ruler" to monitor structural changes of the ion channel that either increase or decrease the distance between donor and acceptor. Single molecule fluorescence anisotropy measures the changing polarization direction of an emitting fluorophore and can be used to determine torsional (twisting) motion of the $5HT_3$ receptor. Finally because fluorescence lifetimes are highly sensitive to local chemical environments, these probes can be used to monitor changes in hydrophobicity, pH, and ionic strength, to name just a few. Using a patch clamp configuration, ion channel currents will be measured in response to serotonin or other agonist binding to the receptor, detailing the kinetics of channel opening and closing. All these experiments can be done at a single molecule level.

II. Experimental

(A) Serotonin Agonist Labeling.

Ni-NTA-R6G for fluorescence labeling of $5HT_3$ Receptor surface via His_6 tag:

1) NTA-lysine was dissolved in 0.1M $NiCl_2$ (pH adjusted to 8 with NaOH).
2) Evaporation of water leaves Ni^{2+}-NTA-lysine crystals.
3) R6G-SE (Molecular Probes) was added to 5 equivalents of Ni^{2+}-NTA-lysine in 50mM $NaHCO_3$, pH 9 with 50% acetonitrile and incubated in the dark at room temperature overnight.
4) Purification was performed using preparatory TLC (silica gel 60) eluting with $CHCl_3/CH_3OH/H_2O$=65/24/4 (R_f=0.27).
5) Extraction with acetonitrile/H_2O=1/1.

Fluorescence labeling of $5HT_3$ Receptor agonists:

An identical procedure is being carried out for 5HT and 2-Me-5HT. The goal is to attach fluorophores with and without covalent spacers to the indole nitrogen, as it is believed that the primary amine and alcohol groups are responsible for ligand binding to the $5HT_3$ receptor.

1) Extract free base: Dissolve agonist in nanopure water, add saturated $NaHCO_3$, extract with $CHCl_3$, and recrystallize.
2) Protect primary amine: Dissolve agonist and phthalic anhydride (1/1) in $CHCl_3$ and reflux at 70C for 16 hours.
3) Protect alcohol: Add stoichiometric amount of TBS at room temperature and stir for 1 hour.
4) Purify via flash chromatography in $CHCl_3$. Produces a light yellow band.
5) Separate into 2 fractions: 1 for introduction of spacer, one without a spacer.
6) Introduction of spacer: solubilize the protected agonist in $CHCl_3$, add 1 equivalent of 2-bromoethylamine, stir at room temperature for 4 hours.
7) Purify via flash chromatography in $CHCl_3$.
8) Introduce R6G-SE (Molecular Probes) to 3 equivalenants of protected dye and 1 equivalent CH_3ONa in CH_3OH. Stir at room temp for 15 minutes, then protect from light and store at 4°C for 6 hours. Add stop reagent: 0.3ml 1.5M hydroxylamine pH 8.5.
9) Purify via preparatory TLC with $CHCl_3/CH_3OH/H_2O/DMF$=64/24/8/4 (R_f=0.3).
10) Remove phthalimide protecting group via hydrazinolysis.

11) Remove TBS protecting group with acetic acid buffered tert-butylammonium fluoride in THF at 0°C for 1 hour.

12) Purify via preparatory TLC as above (R_f=0.2)

(B) Mutagenesis of the $5HT_3$ Serotonin Receptor. The technical goal here was to insert a 6x Histidine (His)-tag at the C-terminus end of the serotonin receptor such that recombinant protein could be purified by Ni-NTA chelate chromatography. A clone containing the 1464-bp $5HT_3$ serotonin receptor gene sequence was graciously provided by Dr. Tina Machu (Texas Tech University). A plasmid map of the original $5HT_3$ clone is provided in Figure2. The overall strategy to accomplish the 6x His-tag insertion involved using site directed mutagenesis (SDM) to create a unique *Bam*HI restriction endonuclease site at the 3' end of the serotonin gene sequence, which would subsequently be used along with the *Not*I site to introduce a short DNA oligomer containing the 6x His-tag. These restriction endonucleases were selected based on the production of 5' overhangs that can be used for directional insertion of DNA oligomers.

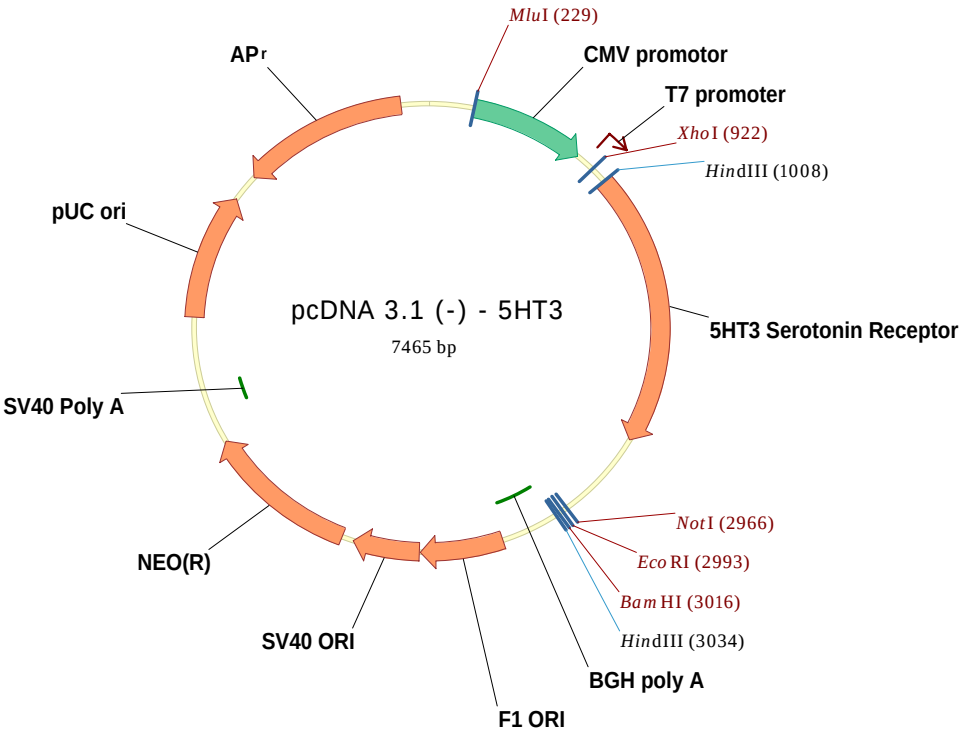

Figure 2. Plasmid map of the pCDNA3.1-5HT3 construct.

In the first step, SDM was used to delete the *Bam*HI restriction endonuclease site (3016) from the vector. SDM was performed using QuikChange® II XL Site-Directed Mutagenesis Kit (Stratagene, La Jolla, CA), which uses a polymerase chain reaction (PCR)-based method to amplify mutated DNA. The primers for this SDM deletion were
5'-CCACACTGGACTAGTGGTTCCGAGCTCGGTACCAAGC-3' (Forward), and
5'-GCTTGGTACCGAGCTCGGAACCACTAGTCCAGTGTGG-3' (Reverse).
Un-mutated, template DNA was removed by restriction digest with *Dpn*I. The mutated DNA was then used to transform XL10-Gold® ultracompetent cells (Stratagene, La Jolla, CA). Restriction digest and agarose gel electrophoresis were used to confirm the deletion of this site (Figure 3).

Figure 3. Restriction digest of *Bam*HI deletion plasmid. Lane 1 (leftmost) is the 1Kb DNA Ladder. Lane 2 is the parental plasmid after digest, showing a linear band. Lanes 3,4, and 5 are the digested mutant plasmids, showing the characteristic 3 lanes for uncut, nicked, and supercoiled plasmid forms, confirming the deletion of the *Bam*HI site (i.e. no linear band).

The second SDM was performed as described above, and used to introduce a unique *Bam*HI site in the $5HT_3$ sequence at 2457 bp. The primers used for this mutation were
5'-CCCTGGTCACTCTCGGATCCATTTGGCATTATTCTTGA-3' (Forward), and
5'-TCAAGAATAATGCCAAATGGATCCGAGAGTGACCAGGG-3' (Reverse). This mutation also resulted in an amino change from Trp481 to Gly481. Clones were screened by restriction digest and agarose gel electrophoresis to confirm the presence of the new *Bam*HI site (Figure 4). The double mutated plasmid was then digested with *Bam*HI and *Not*I, and separated by gel electrophoresis (Figure 5). The ~7,000 bp was excised from the agarose gel using a razor blade, and purified using the QIAquick Gel Extraction Kit (Qiagen, Valencia, CA).

Figure 4. Restriction digest of *Bam*HI mutant plasmid. Lane 6 (rightmost) is the 1Kb DNA Ladder. Lane 5 is the parental plasmid $5HT_3$ after digest, showing a linear band. Lane 4 is the plasmid with *Bam*HI deletion. Lane 3 shows the *Bam*HI mutant without digestion, while lanes 1 and 2 are the digested mutant plasmids, showing the linear bands confirming the addition of a new *Bam*HI site.

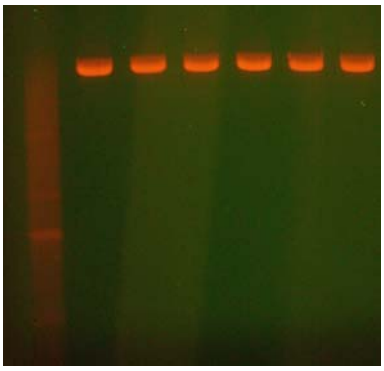

Figure 5. Double restriction digest of *Bam*HI mutant plasmid. Lane 1 (leftmost) is the 1Kb DNA Ladder. Lanes 2-7 are the digested plasmid, showing two bands, one for the uncut plasmid and one for the double cut plasmid, which is missing a 500 bp region. The band for the 500 bp region was not visible in the photograph, but was clear to the eye.

Before ligating the 6x His-tag into the excised plasmid, the His-tag oligomer was phosphorylated using T4 Polynucleotide Kinase (Invitrogen, Carlsbad, CA) in order to increase ligation efficiency. The His-tag oligomers (His codons are underlined) were 5'-GATCCATTTGGCATTATTCTCATCACCATCACCATCACTGAGC-3' (Forward) and 5'-GGCCGCTCAGTGATGGTGATGGTGATGAGAATAATGCCAAATG-3'(Reverse). The ligation was performed using Clonables™ 2X Ligation Premix (EMD Bioscience, San Diego, CA) according the manufacturer's recommendations. The ligated DNA was then transformed into XL10-Gold® ultracompetent cells. Colonies were then selected and sequenced to confirm the mutations and insertion of the 6x His-tag. The final $5HT_3$ construct (pcDNA3.1-$5HT_3$H) is shown in Figure 6. Isolated plasmid DNA was subsequently digested with *Bgl*II, gel extracted, and purified for stable transfection of HEK293-F cells.

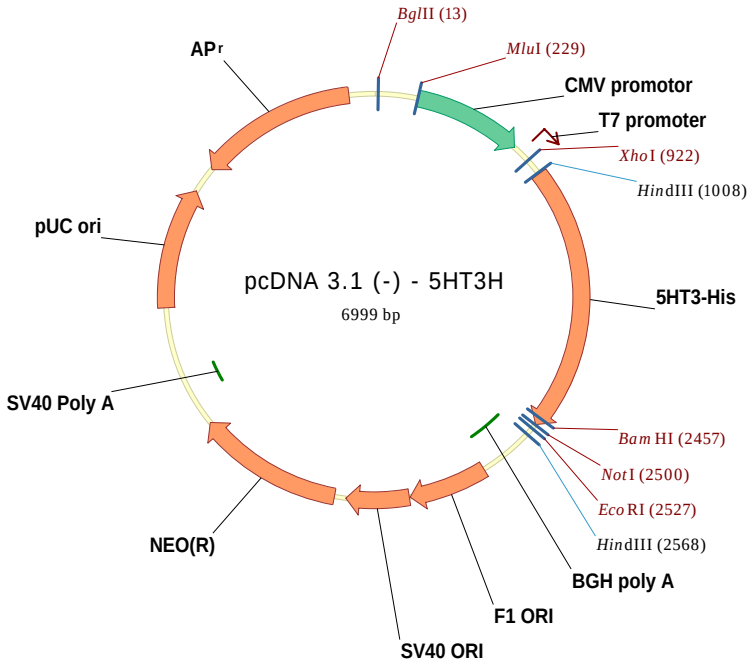

Figure 6. Plasmid map of the 5HT3 His-tagged construct.

(C) Expression of Serotonin Receptor in HEK293-F Cells

Cell Culture: HEK293-F Cells (and all reagents) were obtained from Invitrogen Corporation (Carlsbad, California). The cells were thawed and cultured in suspension in 293 SFM II media supplemented with Glutamax®. All cultures were grown in an incubator at 37°C with 8% CO_2 and a humidified atmosphere in 250mL Erlenmeyer flasks while shaking at 125rpm. During logarithmic growth, $3x10^5$ cells/mL were seeded into 18mL of Freestyle™ 293 Expression Medium and grown overnight. The cells were then concentrated by allowing them to settle to the bottom of the flask and pipetting off some of the media. Subsequently, $1.1x10^6$ cells/mL were transferred into a six-well plate, 1mL per well. Cells were again allowed to settle. Transfection then proceeded.

Transfection: For the transfection, 1 g of digested DNA was suspended in 34 L of Freestyle media. In separate tubes, 1, 2, and 3 L of Lipofectamine 2000® were each diluted in 34 L of Freestyle media and allowed to incubate for 5 minutes at room temperature. The diluted DNA and diluted Lipofectamine were then combined and incubated for 30 minutes at room temperature (1 g DNA for each Lipofectamine sample, to make 68 L total with 1:1, 1:2, and 1:3 DNA:lipid ratios). The mixture was then pipetted gently on the surface of the media of one

well of HEK cells, so that the cells were not disturbed. The lipid-DNA complexes then settled on the cells and the DNA was taken into the cells, where it was integrated into the host genome and could be transcribed and translated. The transfected cells were allowed to grow for 2 days before selection began. The expression vector (see Figure 6) contains a sequence that makes the HEK cells resistant to the antibiotic Geneticin® (neomycin derivative). Upon addition of Geneticin® to the culture media, only the cells that successfully integrated the vector survived. Cells were selected for 8 days before they were deemed stable.

Receptor detection: In order to screen the cells for expression, one can either test *in vivo* or purify the protein and detect it immunologically. For our system, *in vivo* detection is the best option. To do this, NTA-rhodamine was synthesized and will be incubated with the cells for 15 minutes. The cells will then be washed twice with fresh media and dropped onto a slide. The NTA-rhodamine should bind to the His tag on the protein. Using an Olympus IX-70 confocal microscope, mercury lamp and a rhodamine emission filter, the cells will be observed for expression. Non-transfected cells will be examined for background and control, and transfected cells should emit bright red.

III. Future work

Assuming stable expression is achieved, protein purification can begin. The cells will be lysed and the membrane fraction separated and solubilized in nonethylene-glycol monododecyl ether ($C_{12}E_9$). This fraction will then be incubated with the Ni-NTA agarose and washed to remove undesired components. The receptor will then be eluted using imidazole, which has an extremely high binding affinity for the NTA. Purified receptor will be reconstituted into a lipid bilayer of known composition and used for spectroscopic and electrochemical study.

pcDNA3.1-5HT$_3$H DNA sequence

```
                BglII
                ~~~~~~
   1    GACGGATCGG GAGATCTCCC GATCCCCTAT GGTGCACTCT CAGTACAATC

  51    TGCTCTGATG CCGCATAGTT AAGCCAGTAT CTGCTCCCTG CTTGTGTGTT

 101    GGAGGTCGCT GAGTAGTGCG CGAGCAAAAT TTAAGCTACA ACAAGGCAAG

 151    GCTTGACCGA CAATTGCATG AAGAATCTGC TTAGGGTTAG GCGTTTTGCG

                                  MluI
```

```
                                ~~~~~~~
201    CTGCTTCGCG ATGTACGGGC CAGATATACG CGTTGACATT GATTATTGAC
251    TAGTTATTAA TAGTAATCAA TTACGGGGTC ATTAGTTCAT AGCCCATATA
301    TGGAGTTCCG CGTTACATAA CTTACGGTAA ATGGCCCGCC TGGCTGACCG
351    CCCAACGACC CCCGCCCATT GACGTCAATA ATGACGTATG TTCCCATAGT
401    AACGCCAATA GGGACTTTCC ATTGACGTCA ATGGGTGGAG TATTTACGGT
451    AAACTGCCCA CTTGGCAGTA CATCAAGTGT ATCATATGCC AAGTACGCCC
501    CCTATTGACG TCAATGACGG TAAATGGCCC GCCTGGCATT ATGCCCAGTA
551    CATGACCTTA TGGGACTTTC CTACTTGGCA GTACATCTAC GTATTAGTCA
601    TCGCTATTAC CATGGTGATG CGGTTTTGGC AGTACATCAA TGGGCGTGGA
651    TAGCGGTTTG ACTCACGGGG ATTTCCAAGT CTCCACCCCA TTGACGTCAA
701    TGGGAGTTTG TTTTGGCACC AAAATCAACG GGACTTTCCA AAATGTCGTA
751    ACAACTCCGC CCCATTGACG CAAATGGGCG GTAGGCGTGT ACGGTGGGAG
801    GTCTATATAA GCAGAGCTCT CTGGCTAACT AGAGAACCCA CTGCTTACTG
851    GCTTATCGAA ATTAATACGA CTCACTATAG GGAGACCCAA GCTGGCTAGC
                          XhoI
                         ~~~~~~
901    GTTTAAACGG GCCCTCTAGA CTCGAGATCC ATTGTGCTCT AAAGGCAGGC
951    TGGCAGTCTG GGGGACTCAT CCTGAGTGGC TGCTCTGAGG CCCTCCCACA
         HindIII
         ~~~~~~~
1001   TCTGGGAAGC TTGCCATGCG GCTCTGCATC CCGCAGGTGC TGTTGGCCTT
1051   GTTCCTTTCC ATGCTGACAG CCCCGGGAGA AGGCAGCCGG AGGAGGGCCA
1101   CCCAGGAGGA TACCACCCAG CCTGCTCTAC TAAGGCTGTC AGACCACCTC
1151   CTGGCTAACT ACAAGAAGGG GGTGCGGCCT GTGCGGGACT GGAGGAAGCC
1201   TACTACTGTC TCCATTGATG TCATCATGTA TGCCATCCTC AACGTGGATG
1251   AGAAGAACCA GGTTCTGACC ACCTACATAT GGTACCGGCA GTACTGGACT
1301   GATGAGTTTC TGCAGTGGAC TCCTGAGGAC TTCGACAATG TCACCAAATT
1351   GTCCATCCCC ACAGACAGCA TCTGGGTCCC TGACATTCTC ATCAATGAGT
1401   TTGTGGACGT GGGGAAGTCT CCGAACATTC CTTATGTGTA CGTGCATCAT
1451   CGAGGTGAAG TTCAGAACTA CAAGCCCTTG CAATTGGTGA CCGCCTGTAG
```

```
1501    CCTTGACATC TACAACTTCC CCTTTGATGT GCAGAACTGT TCTCTGACTT

1551    TCACCAGCTG GCTGCACACC ATCCAGGACA TCAACATTAC TCTGTGGCGA

1601    TCACCGGAAG AAGTGAGGTC TGACAAGAGC ATCTTCATAA ATCAGGGCGA

1651    GTGGGAGCTG CTGGAGGTGT TCCCCCAGTT CAAGGAGTTC AGCATAGATA

1701    TCAGTAACAG CTATGCAGAA ATGAAGTTCT ACGTGATCAT CCGCCGGAGG

1751    CCTTTATTCT ATGCAGTCAG CCTCTTGCTG CCCAGTATCT TCCTCATGGT

1801    CGTGGACATT GTGGGCTTTT GCCTGCCCCC GGACAGTGGT GAGAGAGTCT

1851    CTTTCAAGAT CACACTCCTT CTGGGATACT CAGTCTTCCT CATCATCGTG

1901    TCAGACACAC TGCCGGCAAC GATCGGTACC CCCCTCATTG GTGTCTACTT

1951    TGTGGTGTGC ATGGCTCTGC TAGTGATAAG CCTCGCTGAG ACCATCTTCA

2001    TTGTGCGGCT GGTGCATAAG CAGGACCTAC AGCGGCCAGT ACCTGACTGG

2051    CTGAGGCACC TGGTCCTAGA CAGAATAGCC TGGATACTCT GCCTAGGGGA

2101    GCAGCCTATG GCCCATAGAC CCCCAGCCAC CTTCCAAGCC AACAAGACTG

2151    ATGACTGCTC AGGTTCTGAT CTTCTTCCAG CCATGGGAAA CCACTGCAGC

2201    CATGTTGGAG GACCTCAGGA CTTGGAGAAG ACCCCAAGGG GCAGAGGTAG

2251    CCCTCTTCCA CCACCAAGGG AGGCCTCACT GGCTGTGCGT GGTCTCTTGC

2301    AAGAGCTATC CTCCATCCGC CACTTCCTGG AGAAGCGGGA TGAGATGCGG

2351    GAGGTGGCAA GGGACTGGCT GCGGGTGGGA TACGTGCTGG ACAGGCTGCT

2401    GTTCCGCATC TACCTGCTGG CTGTGCTCGC TTACAGCATC ACCCTGGTCA

          BamHI                                          NotI
          ~~~~~~~                                        ~~~
2451    CTCTCGGATC CATTTGGCAT TATTCTCATC ACCATCACCA TCACTGAGCG

    NotI                        EcoRI
    ~~~~~                       ~~~~~~~
2501    GCCGCCACTG TGCTGGATAT CTGCAGAATT CCACCACACT GGACTAGTGG

                   HindIII
                   ~~~~~~~
2551    TTCCGAGCTC GGTACCAAGC TTAAGTTTAA ACCGCTGATC AGCCTCGACT

2601    GTGCCTTCTA GTTGCCAGCC ATCTGTTGTT TGCCCCTCCC CCGTGCCTTC

2651    CTTGACCCTG GAAGGTGCCA CTCCCACTGT CCTTTCCTAA TAAAATGAGG

2701    AAATTGCATC GCATTGTCTG AGTAGGTGTC ATTCTATTCT GGGGGGTGGG
```

```
2751    GTGGGGCAGG ACAGCAAGGG GGAGGATTGG GAAGACAATA GCAGGCATGC
2801    TGGGGATGCG GTGGGCTCTA TGGCTTCTGA GGCGGAAAGA ACCAGCTGGG
2851    GCTCTAGGGG GTATCCCCAC GCGCCCTGTA GCGGCGCATT AAGCGCGGCG
2901    GGTGTGGTGG TTACGCGCAG CGTGACCGCT ACACTTGCCA GCGCCCTAGC
2951    GCCCGCTCCT TTCGCTTTCT TCCCTTCCTT TCTCGCCACG TTCGCCGGCT
3001    TTCCCCGTCA AGCTCTAAAT CGGGGGCTCC CTTTAGGGTT CCGATTTAGT
3051    GCTTTACGGC ACCTCGACCC CAAAAAACTT GATTAGGGTG ATGGTTCACG
3101    TAGTGGGCCA TCGCCCTGAT AGACGGTTTT TCGCCCTTTG ACGTTGGAGT
3151    CCACGTTCTT TAATAGTGGA CTCTTGTTCC AAACTGGAAC AACACTCAAC
3201    CCTATCTCGG TCTATTCTTT TGATTTATAA GGGATTTTGC CGATTTCGGC
3251    CTATTGGTTA AAAAATGAGC TGATTTAACA AAAATTTAAC GCGAATTAAT
3301    TCTGTGGAAT GTGTGTCAGT TAGGGTGTGG AAAGTCCCCA GGCTCCCCAG
3351    CAGGCAGAAG TATGCAAAGC ATGCATCTCA ATTAGTCAGC AACCAGGTGT
3401    GGAAAGTCCC CAGGCTCCCC AGCAGGCAGA AGTATGCAAA GCATGCATCT
3451    CAATTAGTCA GCAACCATAG TCCCGCCCCT AACTCCGCCC ATCCCGCCCC
3501    TAACTCCGCC CAGTTCCGCC CATTCTCCGC CCCATGGCTG ACTAATTTTT
3551    TTTATTTATG CAGAGGCCGA GGCCGCCTCT GCCTCTGAGC TATTCCAGAA
3601    GTAGTGAGGA GGCTTTTTTG GAGGCCTAGG CTTTTGCAAA AAGCTCCCGG
3651    GAGCTTGTAT ATCCATTTTC GGATCTGATC AAGAGACAGG ATGAGGATCG
3701    TTTCGCATGA TTGAACAAGA TGGATTGCAC GCAGGTTCTC CGGCCGCTTG
3751    GGTGGAGAGG CTATTCGGCT ATGACTGGGC ACAACAGACA ATCGGCTGCT
3801    CTGATGCCGC CGTGTTCCGG CTGTCAGCGC AGGGGCGCCC GGTTCTTTTT
3851    GTCAAGACCG ACCTGTCCGG TGCCCTGAAT GAACTGCAGG ACGAGGCAGC
3901    GCGGCTATCG TGGCTGGCCA CGACGGGCGT TCCTTGCGCA GCTGTGCTCG
3951    ACGTTGTCAC TGAAGCGGGA AGGGACTGGC TGCTATTGGG CGAAGTGCCG
4001    GGGCAGGATC TCCTGTCATC TCACCTTGCT CCTGCCGAGA AAGTATCCAT
4051    CATGGCTGAT GCAATGCGGC GGCTGCATAC GCTTGATCCG GCTACCTGCC
4101    CATTCGACCA CCAAGCGAAA CATCGCATCG AGCGAGCACG TACTCGGATG
4151    GAAGCCGGTC TTGTCGATCA GGATGATCTG GACGAAGAGC ATCAGGGGCT
```

```
4201    CGCGCCAGCC GAACTGTTCG CCAGGCTCAA GGCGCGCATG CCCGACGGCG
4251    AGGATCTCGT CGTGACCCAT GGCGATGCCT GCTTGCCGAA TATCATGGTG
4301    GAAAATGGCC GCTTTTCTGG ATTCATCGAC TGTGGCCGGC TGGGTGTGGC
4351    GGACCGCTAT CAGGACATAG CGTTGGCTAC CCGTGATATT GCTGAAGAGC
4401    TTGGCGGCGA ATGGGCTGAC CGCTTCCTCG TGCTTTACGG TATCGCCGCT
4451    CCCGATTCGC AGCGCATCGC CTTCTATCGC CTTCTTGACG AGTTCTTCTG
4501    AGCGGGACTC TGGGGTTCGA AATGACCGAC CAAGCGACGC CCAACCTGCC
4551    ATCACGAGAT TTCGATTCCA CCGCCGCCTT CTATGAAAGG TTGGGCTTCG
4601    GAATCGTTTT CCGGGACGCC GGCTGGATGA TCCTCCAGCG CGGGGATCTC
4651    ATGCTGGAGT TCTTCGCCCA CCCCAACTTG TTTATTGCAG CTTATAATGG
4701    TTACAAATAA AGCAATAGCA TCACAAATTT CACAAATAAA GCATTTTTTT
4751    CACTGCATTC TAGTTGTGGT TTGTCCAAAC TCATCAATGT ATCTTATCAT
4801    GTCTGTATAC CGTCGACCTC TAGCTAGAGC TTGGCGTAAT CATGGTCATA
4851    GCTGTTTCCT GTGTGAAATT GTTATCCGCT CACAATTCCA CACAACATAC
4901    GAGCCGGAAG CATAAAGTGT AAAGCCTGGG GTGCCTAATG AGTGAGCTAA
4951    CTCACATTAA TTGCGTTGCG CTCACTGCCC GCTTTCCAGT CGGGAAACCT
5001    GTCGTGCCAG CTGCATTAAT GAATCGGCCA ACGCGCGGGG AGAGGCGGTT
5051    TGCGTATTGG GCGCTCTTCC GCTTCCTCGC TCACTGACTC GCTGCGCTCG
5101    GTCGTTCGGC TGCGGCGAGC GGTATCAGCT CACTCAAAGG CGGTAATACG
5151    GTTATCCACA GAATCAGGGG ATAACGCAGG AAAGAACATG TGAGCAAAAG
5201    GCCAGCAAAA GGCCAGGAAC CGTAAAAAGG CCGCGTTGCT GGCGTTTTTC
5251    CATAGGCTCC GCCCCCCTGA CGAGCATCAC AAAAATCGAC GCTCAAGTCA
5301    GAGGTGGCGA AACCCGACAG GACTATAAAG ATACCAGGCG TTTCCCCCTG
5351    GAAGCTCCCT CGTGCGCTCT CCTGTTCCGA CCCTGCCGCT TACCGGATAC
5401    CTGTCCGCCT TTCTCCCTTC GGGAAGCGTG GCGCTTTCTC ATAGCTCACG
5451    CTGTAGGTAT CTCAGTTCGG TGTAGGTCGT TCGCTCCAAG CTGGGCTGTG
5501    TGCACGAACC CCCCGTTCAG CCCGACCGCT GCGCCTTATC CGGTAACTAT
5551    CGTCTTGAGT CCAACCCGGT AAGACACGAC TTATCGCCAC TGGCAGCAGC
```

```
5601    CACTGGTAAC AGGATTAGCA GAGCGAGGTA TGTAGGCGGT GCTACAGAGT
5651    TCTTGAAGTG GTGGCCTAAC TACGGCTACA CTAGAAGAAC AGTATTTGGT
5701    ATCTGCGCTC TGCTGAAGCC AGTTACCTTC GGAAAAAGAG TTGGTAGCTC
5751    TTGATCCGGC AAACAAACCA CCGCTGGTAG CGGTTTTTTT GTTTGCAAGC
5801    AGCAGATTAC GCGCAGAAAA AAAGGATCTC AAGAAGATCC TTTGATCTTT
5851    TCTACGGGGT CTGACGCTCA GTGGAACGAA AACTCACGTT AAGGGATTTT
5901    GGTCATGAGA TTATCAAAAA GGATCTTCAC CTAGATCCTT TTAAATTAAA
5951    AATGAAGTTT TAAATCAATC TAAAGTATAT ATGAGTAAAC TTGGTCTGAC
6001    AGTTACCAAT GCTTAATCAG TGAGGCACCT ATCTCAGCGA TCTGTCTATT
6051    TCGTTCATCC ATAGTTGCCT GACTCCCCGT CGTGTAGATA ACTACGATAC
6101    GGGAGGGCTT ACCATCTGGC CCCAGTGCTG CAATGATACC GCGAGACCCA
6151    CGCTCACCGG CTCCAGATTT ATCAGCAATA AACCAGCCAG CCGGAAGGGC
6201    CGAGCGCAGA AGTGGTCCTG CAACTTTATC CGCCTCCATC CAGTCTATTA
6251    ATTGTTGCCG GGAAGCTAGA GTAAGTAGTT CGCCAGTTAA TAGTTTGCGC
6301    AACGTTGTTG CCATTGCTAC AGGCATCGTG GTGTCACGCT CGTCGTTTGG
6351    TATGGCTTCA TTCAGCTCCG GTTCCCAACG ATCAAGGCGA GTTACATGAT
6401    CCCCCATGTT GTGCAAAAAA GCGGTTAGCT CCTTCGGTCC TCCGATCGTT
6451    GTCAGAAGTA AGTTGGCCGC AGTGTTATCA CTCATGGTTA TGGCAGCACT
6501    GCATAATTCT CTTACTGTCA TGCCATCCGT AAGATGCTTT TCTGTGACTG
6551    GTGAGTACTC AACCAAGTCA TTCTGAGAAT AGTGTATGCG GCGACCGAGT
6601    TGCTCTTGCC CGGCGTCAAT ACGGGATAAT ACCGCGCCAC ATAGCAGAAC
6651    TTTAAAAGTG CTCATCATTG GAAAACGTTC TTCGGGGCGA AAACTCTCAA
6701    GGATCTTACC GCTGTTGAGA TCCAGTTCGA TGTAACCCAC TCGTGCACCC
6751    AACTGATCTT CAGCATCTTT TACTTTCACC AGCGTTTCTG GGTGAGCAAA
6801    AACAGGAAGG CAAAATGCCG CAAAAAAGGG AATAAGGGCG ACACGGAAAT
6851    GTTGAATACT CATACTCTTC CTTTTTCAAT ATTATTGAAG CATTTATCAG
6901    GGTTATTGTC TCATGAGCGG ATACATATTT GAATGTATTT AGAAAAATAA
6951    ACAAATAGGG GTTCCGCGCA CATTTCCCCG AAAAGTGCCA CCTGACGTC
```

Transducer Development (work in progress)

Design of Miniaturized Electrochemically and Optically-Addressable Platforms for Single Molecule Detection

Ryan W. Davis[†], Jeb H. Flemming[‡], Susan M. Brozik[‡] and James A. Brozik[†]**

[†]Department of Chemistry, The University of New Mexico, Albuquerque, NM 87131

[‡] Microsensor Science and Technology, Sandia National Laboratories, Albuquerque, NM 87185-0892

Abstract

A chip-based platform designed for protein/bilayer assembly was fabricated using electron beam lithography. 50-500 nm holes were etched in a silicon nitride (SiN) membrane. For this process 400 micron, 1-0-0 plane, silicon wafers with 1 micron of low stress, high density, SiN coated on each side was used. Electrodes consisting of 20 nm of chromium and 100 nm of silver were then defined on the top of the wafer using thermal evaporation. In order to measure the current from the electrodes, a housing device was fabricated using polyetheretherketone (PEEK). Some of these devices have been tested and show good performance for tight membrane seals for electrochemical measurements. For the spectroscopic characterization on the same chip, 1-10 micron diameter holes were fabricated. Experimental results show that the 10 micron sized pores provide the best seals for bilayer assembly and single molecule measurements.

I. Introduction

Our long term goal of this project will be an ion channel-based sensor platform/array designed to detect specific targets based on the transduction of biological molecular recognition/binding events to time dependent electronic and optical signatures. Ion channel systems will be patterned on optically and electrochemically addressable fluidic platforms to provide for specific molecular recognition or (less specific) adsorption of several classes of target molecules, e.g. toxins, proteins, and oligonucleotides. Transduction of binding/adsorption into a characteristic digital electronic signature will depend on how the binding event modulates the magnitude and frequency of the temporal current fluctuations as well as the specific structural states of the channel protein.

In 1997, Cornell et al.[1], demonstrated the feasibility of an electrode-supported gated ion channel based sensor. They devised a multi-step assembly procedure to tether a lipid bilayer containing gramicidin ion channels linked to antibodies to a gold electrode surface. Such a tethered configuration is of interest in general for an ion-channel-based sensor because it creates an ionic reservoir between the electrode and membrane and serves to maintain the bilayer fluidity and facilitate the incorporation of membrane proteins. In the presence of an applied potential, ions flow between the reservoir and the external fluid when the channels are conductive/open. Upon antibody binding to a target analyte, the gramicidin residing in the upper leaflet is displaced laterally, 'switching off' the ion current and resulting in a reduction in conductance of up to 40%. This sensor system suffers however from several serious problems including the stability of the tethered bilayer and the complexity of the synthetic chemistry and its reproducibility.

More recently, Hagen Bayley and co-workers have developed an alternate ion channel based sensing scheme[2-5] coined 'stochastic sensing' that relies on analysis of the temporal fluctuations of ion channel currents in α-haemolysin (αHL) pores prepared as black lipid membranes. The natural ion current fluctuations are modulated by reversible analyte binding, allowing in principle the monitoring of individual binding events. In stochastic sensing the frequency of these binding events is related to the concentration of analyte, while the amplitude and duration of the current modulation depend on the identity of the analyte. Thus far these types of sensor have yet to be fabricated in chip-based arrays because of the bilayer instability.

The positioning of lipid vesicles on planar chip-based platforms presents unique challenges in circuit integration, materials compatibility, high electrical insulation (tight membrane seals), and electrokinetic effects in surface micromachined silicon. Microchip-based techniques for analysis of single ion channels have been reported[6,7] but to date the fluidic platforms have not incorporated multiple recording sites integrated with on chip electronics nor do they include micro-optics for simultaneous electrochemical and optical analysis. Efforts from our team thus far have utilized micro-machined fluidic platforms with electrical and optical input/output. The current platforms provide for patch clamp electronic analysis with microfabricated electrodes and spatially resolved optical addressability (we have yet to miniaturize the optics nor is the fluidic chip designed in an array configuration needed for sensing applications).

II. Experimental

In order to suspend a lipid bilayer in a stable environment that can be both optically and electrically interrogated, two devices have been designed and fabricated using silicon. Both devices use the same operating principle. The topside of the device contains two isolated Teflon reservoirs. The reservoirs are connected to the bottom side by etching vias, small holes, through the wafer. The backside of the wafer contains a microfluidic channel connecting the two reservoirs. Electrical measurements are made with on-chip silver electrodes.

(A) Fabrication of Single Molecule Detection Platform using Bosch Process.

The first device, Figure 1, was fabricated using a well-characterized Bosch process, which creates vertical vias with high aspect ratios. For this process phosphate doped, 300 μm thick, 1-0-0 silicon wafers were used. Photoresist was spun onto the topside of the wafer at a thickness of 15 μm and exposed to a pattern. The wafer was then etched through using the Bosch process creating, depending upon the die, two 25, 50, 100, or 200 micron diameter wide cylinders (this allows a uniform lipid bilayer to suspend between the topside and the backside of the wafer). Next, 4330 photoresist was spun onto the backside of the wafer at a thickness of 4.3 μm and patterned. The wafer was

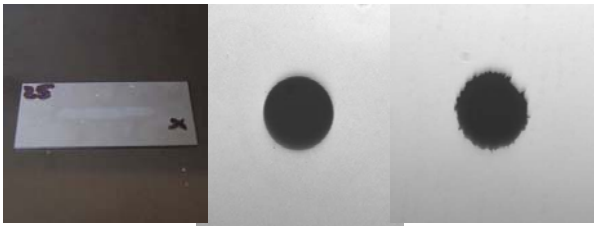

Figure 1. Single molecule detection platform using the Bosch process showing topside and jagged backside of the through hole.

then etched 150 nm deep to create the microfluidic channel connecting the two vias. Although we were able to form tight membrane seals (~15 gigohm resistance), there were several problems with this prototype chip. First, the lipid bilayer was assembling in the middle of the 300 micron thick wafer, 150 microns from the top of the coverslip. Some of our spectroscopic measurements (evanescent excitation) require the bilayer to be within 500 nm of the forward surface of the coverslip. We were also unable to create perfectly uniform cylinders (visible in Figure 1), which led to unstable bilayers. Finally we observed that smaller diameters yielded more stable bilayer formation consequently new fabrication techniques were required for nm pore diameters.

(B) Fabrication of Single Molecule Detection Platform using Electron Beam Lithography.

The second device fabricated (Figure 2 and 3) incorporates a silicon nitride (SiN) membrane with etched sub-micron holes. For this device 110 silicon, 400 microns thick, coated with 1 micron of silicon nitride (SiN) on both sides was used. The wafer was cleaned by an acetone, methanol, and isoproponal rinse. It was then placed in oxygen plasma for five minutes at five watts. The through holes in the bottom side SiN layer, which serve as a transition point

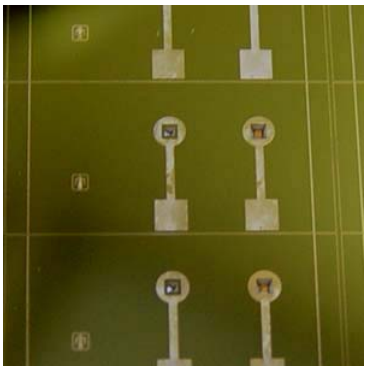

Figure 2. Uncut SMD chip showing on-chip working and counter electrodes.

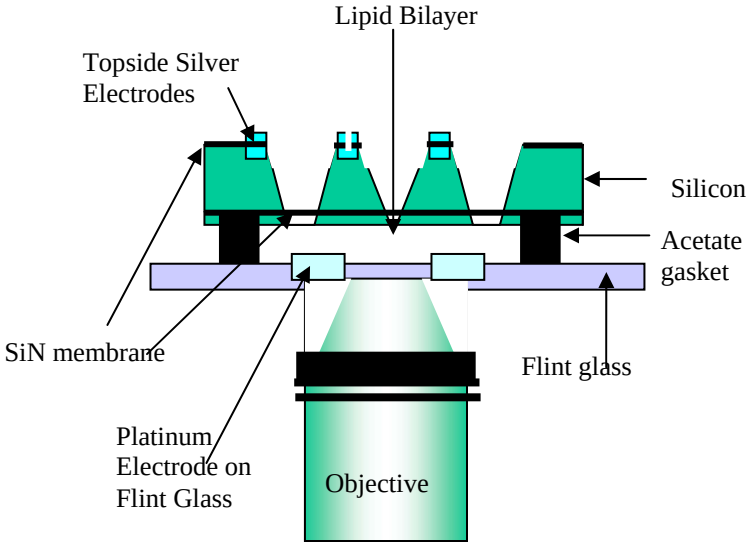

Figure 3. Conceptual diagram of side view of SMD platform and relation to objective.

from the topside of the wafer to the bottom side of the wafer, range from 2 micron to 10 microns and were fabricated by depositing the positive photoresist (PR) AZ 4330 (Clariant) onto the backside of the wafer. The AZ 4330 PR was patterned using a Karl Suss MA6

Contact Aligner and developed with 1:4 AZ 400K photodeveloper (Clariant). The exposed SiN layer was etched in a reactive ion etch process (Vacutec, Plasma Systems) containing CF_4 and O_2 at 100 millitorr for 25 minutes.

The topside electrodes were fabricated using AZ 4330 PR as well. Once patterned and developed, electrodes consisting of 20 nm of chromium and 100 nm of silver were defined on the top of the wafer using thermal evaporation. The SiN on the topside of the wafer, inside the silver electrode, was removed in a reactive ion etch, using the same process described above, to create the through holes in the bottom side SiN. This exposes the underlying silicon. The wafer is then placed in a potassium hydroxide (KOH) bath and allowed to sit for 7 hours at 85^{o}C. The KOH preferentially etches in the <100> plane, creating an anisotropic V-etch, with sidewalls that form a 54.7^{o} angle with the surface. In addition to the silver electrodes fabricated on the topside of the SMD platform, a second counter electrode, fabricated out of platinum, was evaporated onto a flint glass coverslip. This coverslip was then connected to the SMD platform, using 2 mil thick acetate tape.

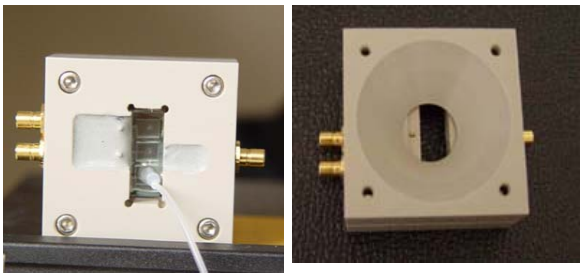

Figure 4. Top side (A) and the bottom side (B) of the housing

In order to measure the current from the electrodes, a housing device has been fabricated using polyetheretherketone (PEEK), Figure 4. The top piece contains three gold pogo pins that contact the single molecule device at various points. The pogo pins output to standard Pasternack plugs that can be easily connected to the electrochemical setup. The bottom piece has a conical cut in the middle that allows the objective to come in direct contact of the flint glass on the bottom of the device.

(C) Fabrication of SMD Platform

- A 400 micron thick silicon wafer

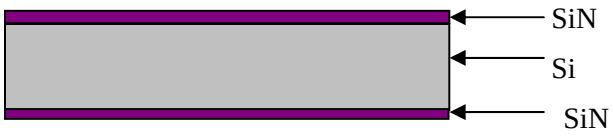

- Pattern and etch pore into topside SiN

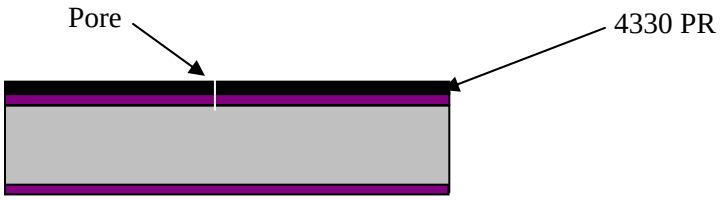

- Pattern and deposit Chrome/Silver for electrodes

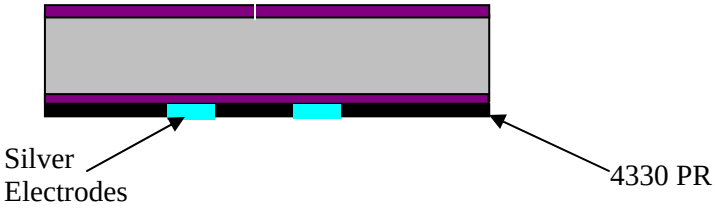

- Pattern and etch backside SiN.

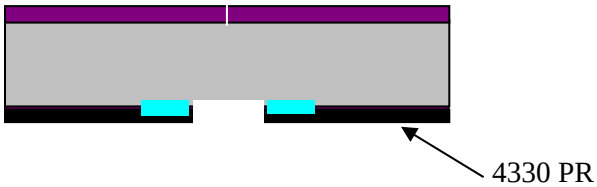

- KOH etch backside to stop on topside SiN membrane

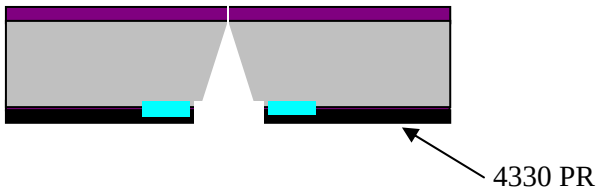

- Final Product

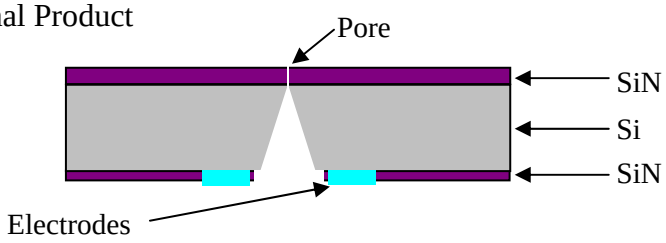

III. References

1. Pace, R.J., et al., *Nature*, **1997**, 387(6633), 580-583.
2. Bayley H., Cremer P.S., *Nature*, **2001**, 413(Sept.13), 226-230.
3. Bayley H., O. Braha, and L.-Q. Gu, *Adv. Mater*., **2000,** 12, 139-142.
4. Gu, L.-Q., et al., *Nature*, **1999**, 398(6729), 686-690.
5. Howorka, S., Cheley S., and Bayley H., *Nature Technology*, **2001,** 19(July), 636-639.
6. Schmidt C., Mayer M., and Vogel H., *Angew. Chem. Int. Ed*, **2000,** *39*, No.17, 3137-3140.
7. Pantoja R., Sigg D., Blunck R., Bezanilla F., and Heath J. R., *Biophysical Journal*, **2001**, 81, 2389-2394.

Distribution

1	MS 0123	Donna Chavez, 1011
1	MS 1425	Stephen Casalnuovo, 1744
10	MS 0892	Susan Brozik, 1744
1	MS 0892	Elizabeth Patrick, 1744
1	MS 1425	Jeb Flemming, 1744
1	MS 0892	Lauren Meyer, 1764
1	MS 1412	George Bachand, 1116
1	MS 1110	Laura Frink, 9212
1	MS 9018	Central Technical Files, 8945-1
2	MS 0899	Technical Library, 9616
10	James Brozik University of New Mexico Department of Chemistry Clark Hall Room 103 Albuquerque, NM 87131	